

AD-A 125 479

DRSAR-LEP-L
Tech Lib

AD

CONTRACT REPORT ARBRL-CR-00504

TECHNICAL
LIBRARY

ON THE DETERMINATION OF THE GAS
TEMPERATURE FROM THE VELOCITY OF THE
MUZZLE RAREFACTION WAVE

Prepared by

Paul Gough Associates, Inc.
P.O. Box 1614
Portsmouth, NH 03801

February 1983



US ARMY ARMAMENT RESEARCH AND DEVELOPMENT COMMAND
BALLISTIC RESEARCH LABORATORY
ABERDEEN PROVING GROUND, MARYLAND

Approved for public release; distribution unlimited.

DTIC QUALITY INSPECTED 3

Destroy this report when it is no longer needed.
Do not return it to the originator.

Additional copies of this report may be obtained
from the National Technical Information Service,
U. S. Department of Commerce, Springfield, Virginia
22161.

The findings in this report are not to be construed as
an official Department of the Army position, unless
so designated by other authorized documents.

*The use of trade names or manufacturers' names in this report
does not constitute indorsement of any commercial product.*

UNCLASSIFIED

SECURITY CLASSIFICATION OF THIS PAGE (When Data Entered)

REPORT DOCUMENTATION PAGE		READ INSTRUCTIONS BEFORE COMPLETING FORM
1. REPORT NUMBER CONTRACT REPORT ARBRL-CR-00504	2. GOVT ACCESSION NO.	3. RECIPIENT'S CATALOG NUMBER
4. TITLE (and Subtitle) ON THE DETERMINATION OF THE GAS TEMPERATURE FROM THE VELOCITY OF THE MUZZLE RAREFACTION WAVE		5. TYPE OF REPORT & PERIOD COVERED Final Report July 81 - May 82
		6. PERFORMING ORG. REPORT NUMBER PGA-TR-82-3
7. AUTHOR(s) P. S. Gough		8. CONTRACT OR GRANT NUMBER(s) DAAK11-81-C-0004
9. PERFORMING ORGANIZATION NAME AND ADDRESS Paul Gough Associates, Inc. P.O. Box 1614 Portsmouth, NH 03801		10. PROGRAM ELEMENT, PROJECT, TASK AREA & WORK UNIT NUMBERS 1L161102AH43
11. CONTROLLING OFFICE NAME AND ADDRESS US Army Armament Research & Development Command US Army Ballistic Research Laboratory (ORDAR-BL) Aberdeen Proving Ground, MD 21005		12. REPORT DATE February 1983
14. MONITORING AGENCY NAME & ADDRESS (if different from Controlling Office)		13. NUMBER OF PAGES 79
		15. SECURITY CLASS. (of this report) UNCLASSIFIED
16. DISTRIBUTION STATEMENT (of this Report) Approved for public release; distribution unlimited.		
17. DISTRIBUTION STATEMENT (of the abstract entered in Block 20, if different from Report)		
18. SUPPLEMENTARY NOTES		
19. KEY WORDS (Continue on reverse side if necessary and identify by block number) Muzzle Blast Muzzle Temperature Speed of Sound		
20. ABSTRACT (Continue on reverse side if necessary and identify by block number) nlg The temperature of the propellant gas as it flows out of the muzzle of a gun is a principal factor in respect to the strength of the air blast which accompanies the discharge of the projectile. The temperature also plays a dominant role in respect to the occurrence of secondary combustion of flash. We discuss the fundamental basis for a method of determining the temperature from measurements of the velocity of the unloading wave or rarefaction created by the discharge of the projectile. The method is, (cont'd on back)		

UNCLASSIFIED

SECURITY CLASSIFICATION OF THIS PAGE(When Data Entered)

of course, restricted to cases in which the projectile velocity is less than the speed of sound in the gas directly behind it.

For charges which are completely burnt and in which the products of combustion at the muzzle are purely gaseous, three sources of error are identified. First, the measurement time may be approximately equal to the relaxation time for changes in chemical composition. This will result in dispersion and since the unloading wave contains components of all frequencies, part of the wave will move with the frozen wave speed and part will move with the equilibrium speed. Due to dissipation the faster frozen components will be less detectable at increasing distances from the muzzle. Second, the unloading wave is not one-dimensional and the radial relaxation time is of the same order as the measurement time. Significant geometrical dispersion will result and will be superimposed on the chemical relaxation. Third, the temperature of the gas in the measurement zone may differ significantly from the space-mean value as a consequence of a non-uniform release of chemical energy by the propellant and the deviation may be to higher or to lower values.

For charges in which the products are two-phase at the muzzle a fourth source of error may arise from dispersion due to two-phase relaxation phenomena

UNCLASSIFIED

SECURITY CLASSIFICATION OF THIS PAGE(When Data Entered)

Foreword

Technical cognizance for the subject contract as a whole has been provided by Mr. A. W. Horst, Jr., U.S. Army Ballistic Research Laboratory DRDAR-BLP, and for Task I, in particular, by Dr. G. Keller, DRDAR-BLP.

The author acknowledges with gratitude the assistance provided by Dr. Keller in the preparation of this report as well as the many helpful comments and criticisms of Drs. J. Heimerl, E. Freedman and E. Schmidt of BRL who reviewed certain sections of the draft version.

TABLE OF CONTENTS

	Page
FOREWORD.....	3
1.0 INTRODUCTION.....	7
1.1 Objectives and Scope of Study.....	7
1.2 Review of Muzzle Flow Phenomena.....	9
2.0 PROPAGATION OF SOUND.....	16
2.1 Speed of Sound in an Ideal Fluid.....	18
2.2 Characteristic Lines.....	22
2.3 Speed of Sound in Real Gases.....	27
2.3.1 Effects of Viscosity and Thermal Conductivity.....	28
2.3.2 Effects of Finite Molecular Relaxation Times.....	31
2.3.2.1 The Mandelshtam-Leontovich Theory of Molecular Relaxation Phenomena.....	32
2.3.2.2 Translational, Rotational and Vibrational Relaxation Times.....	34
2.3.2.3 Chemical Relaxation Times.....	36
2.4 Speed of Sound in Two-Phase Flow.....	40
3.0 PROPAGATION OF THE MUZZLE RAREFACTION WAVE.....	48
4.0 CONCLUSIONS.....	60
REFERENCES.....	62
NOMENCLATURE.....	69
DISTRIBUTION LIST.....	71

1.0 INTRODUCTION

The expulsion of a projectile from the muzzle of a gun is accompanied by the discharge of the propulsion gas into the atmosphere. At the instant of discharge the propulsion gas has a temperature of approximately 1800°K, for a typical high zone howitzer charge, and a pressure of 50 MPa. The release of the gas is sudden and the environmental result is similar to the blast created by an explosion. Moreover, because most solid propellant formulations are fuel-rich, the mixing of the gas with ambient oxygen can result in a significant degree of exothermic reaction with a concomitant increase in the strength of the blast.

The effects of blast and of flash, due to secondary combustion, are always undesirable and in many cases may be sufficiently pronounced as to disqualify a propelling charge from active service. Accordingly, considerable effort has been exerted over the years to understand and control the mechanisms involved in the discharge of the propulsion gas into the atmosphere.

1.1 Objectives and Scope of Study

The particular aspect of this problem which is addressed herein relates to certain attempts to determine the temperature of the propelling gas at the instant of muzzle discharge. Determination of the temperature of the exiting gas is important for two reasons. First, the temperature defines the internal energy, the flux of which is expected to correlate with the strength of the muzzle blast. Second, the temperature is an important parameter in respect to the occurrence of secondary combustion or flash, the result of which is to increase significantly the blast energy.

The method of determining the temperature as described by Schmidt et al¹ is based on detection, by means of pressure gages, of the rearward propagating rarefaction wave which is generated by the expulsion of the projectile. Since such a wave is only generated when the projectile launch velocity is less than the speed of sound in the gas at the base of the projectile, the technique is clearly limited to such cases.

Conceptually, this technique is very simple. As the rearward propagating rarefaction wave passes each of a series of pressure gages located at various axial stations near the breech, a point of inflection or discontinuity of slope is introduced in each of the respective pressure histories. From the time correlation of the data and the known axial spacing of the gages, the wave speed is deduced.

¹Schmidt, E. M., Gion, E. J., and Shear, D. D.

"Acoustic Thermometric Measurements of Propellant Gas Temperatures in Guns"

AIAA J., vol. 15, no. 2, pp. 222-226

February 1977

Eliminating, in some fashion, the contribution of the gas velocity to the wave speed, one has the speed of sound. Thus, given the equation of state of the gas, one may deduce the temperature.

Our purpose here is to examine the assumptions upon which the technique rests. Of particular interest is the influence of non-ideal properties of the gas--at the molecular level--on the rate of propagation of small disturbances. For example, the gas is a multicomponent mixture whose rates of chemical reaction may influence the speed of sound. Also of interest is the influence of what may be viewed as nonideal macroscopic behavior. For example, the unloading wave is not one-dimensional. A finite interval is required for information concerning the discharge of the projectile to reach the centerline of the tube. In addition, the properties of the flow are not uniform over each cross section even prior to the unloading event, due to the existence of thermal and mechanical boundary layers. Nor is the temperature behind the projectile necessarily uniform in the axial direction. Depending on the distribution of the propellant during combustion, an entropy layer may be present and the temperature near the base of the projectile may be either locally elevated or locally depressed. Finally, the flow may not be single-phase. If particulate matter is present, the speed of sound will be affected in some degree.

The scope of our study is as follows. We seek to identify, at least qualitatively, the influence of the nonideal phenomena. Wherever possible, we provide quantitative assessments. However, we do not consider errors due to the accuracy of the instrumentation per se. Nor do we consider the accuracy with which the equation of state itself may be inverted to deduce the temperature from the speed of sound in the absence of dispersive mechanisms.

The balance of this chapter is devoted to a brief summary of the muzzle blast literature in order to provide a suitable perspective for the present study.

In chapter 2.0 we discuss the propagation of sound. The approach taken in chapter 2.0 is to discuss the individual roles played by the nonideal molecular formula and also by the presence of dispersed particulate cloud. We do not attempt to write down an explicit formula for the coupled influence of all the nonidealities acting concurrently. We do, however, identify the frequency domain within which each process becomes active and the corresponding influence on the sound speed.

In chapter 3.0 we discuss the behavior of the muzzle unloading wave and assess the sources of error which may affect the determination of the gas temperature from measurements of the velocity of the unloading wave.

1.2 Review of Muzzle Flow Phenomena

The principal source of energy deposition in the ambient air is, of course, the propellant gas which is expelled following the discharge of the projectile. Prior to the discharge of the projectile, however, the gas ahead of the projectile must be forced out of the tube. Although the energy content of this precursor flow is small by comparison with that in the propellant, the precursor flow exerts a significant influence on the blast pressure which is ultimately created by the propellant flow. This is due to the heating and acceleration of the ambient gas by the precursor flow. Experiments based on normal and evacuated gun tubes have been performed by Schmidt et al² and the maximum near field overpressure has been shown to be reduced by nearly 50% by the presence of the precursor flow.

The structure of the exterior flows created first by the precursor and subsequently by the propellant gas are qualitatively similar. Both comprise an underexpanded jet, bounded laterally by weak shocks and bounded downstream of the muzzle by a strong shock, the Mach disk. The system of shock waves is surrounded by a contact surface which separates the effluent from the ambient gas and this, in turn, is surrounded by a nearly spherical shock or air blast.

Further details of the structure of the exterior flow may be found in the discussions of Oswatitsch,³ Schmidt and Shear,⁴ and Erdos and Del Guidice.⁵ We now abstract some of this discussion, noting that we are considering, for the moment, muzzle flows without secondary combustion, a topic on which we will comment subsequently.

²Schmidt, E. M., Gion, E. J., and Fansler, K. S.
"Analysis of Weapon Parameters Controlling the Muzzle Blast
Overpressure Field"
Fifth International Symposium on Ballistics April 1980

³Oswatitsch, K.
"Intermediate Ballistics"
DVL Report 358, June 1964
Deutschen Versuchsanstalt für Luft und Raumfahrt, Aachen, Germany
AD 473-249

⁴Schmidt, E. M. and Shear, D. D.
"Optical Measurements of Muzzle Blast"
AIAA J., vol. 13, no. 8, pp. 1086-1091 August 1975

⁵Erdos, J. I. and Del Guidice, P. D.
"Calculation of Muzzle Blast Flowfields"
AIAA J., vol. 13, no. 8, pp. 1048-1055 August 1975

While there are great structural similarities between the precursor and the propellant flow fields, differences obviously arise due to the influence, in the latter, of the presence of the projectile and, possibly, the oxidation of the fuel-rich propellant gas. It is therefore of interest to consider first the precursor field and subsequently the propellant gas field. These are illustrated in Figure 1.1.

The acceleration of the projectile drives a compression front through the gas which initially fills the tube. Because of the rapid rate of increase of the projectile velocity, the compression front forms a shock whose emergence from the muzzle initiates the external precursor flow field. The pressure behind the precursor shock is approximately one order of magnitude higher than the ambient pressure. Therefore, the efflux is either initially supersonic, if the projectile velocity is sufficiently high, or else quickly becomes sonic, the large pressure gradient near the muzzle accelerating the fluid in the exit plane to the point at which information no longer travels upstream in the barrel.

It has been observed by Klingenberg⁶ that, in fact, more than one precursor shock can be formed, depending on the motion of the projectile and its interaction with the tube due to the action of the rotating band.

The sudden elevation of the pressure at the exit plane of the tube is transmitted into the ambient atmosphere as a nearly spherical shock. The structure of the flow near the shock front is that of a blast wave, namely, a shock driven by the expanding products of an explosion. More precisely, the behavior is that of a variable energy blast since the muzzle efflux provides a continuing source of energy. Measurements of the blast trajectory, due to the propellant gas flow, along the axis of symmetry of an M16 rifle have been shown to correlate well with the theoretical behavior of a blast having a constant rate of energy addition.⁵ This accords well with the calculations of the rate of energy efflux from the barrel by Schmidt and Shear⁴ using the RECRIF code of Celmins.⁷

⁶Klingenberg, G.

"Investigation of Combustion Phenomena Associated with the Flow of Hot Propellant Gases. III: Experimental Survey of the Formation and Decay of Muzzle Flow Fields and of Pressure Measurements"
Combustion and Flame, vol. 29, no. 3

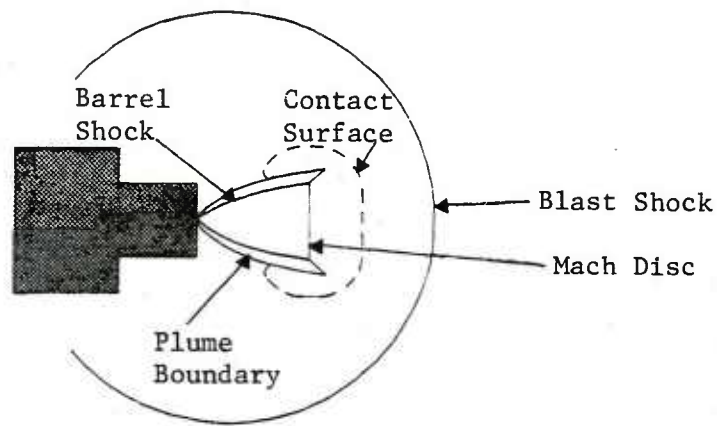
1977

⁷Celmins, A.

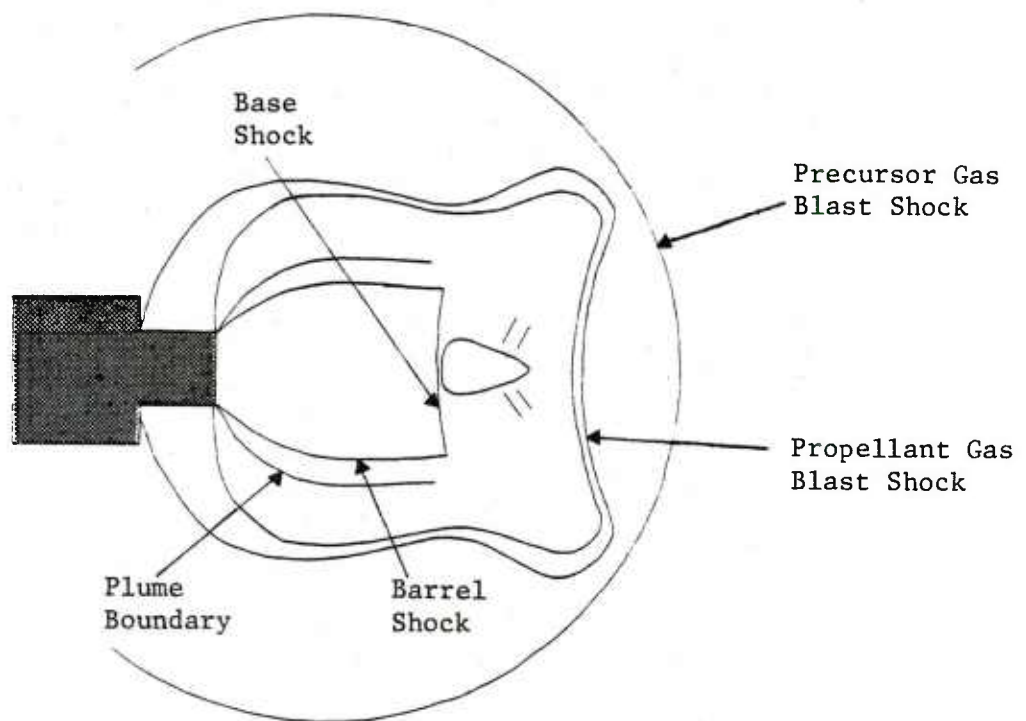
"Theoretical Basis of the Recoilless Rifle Interior Ballistic Code, RECRIF"

Ballistic Research Laboratory Report 1931
(ADB 013832L)

September 1976



Structure of precursor blast field



Structure of propellant gas blast field

Figure 1.1 Structure of Precursor and Propellant Blast Fields
(after Erdos and Del Guidice⁵)

Since, on the one hand, the outflowing plume is the driving mechanism which supports the blast, it follows, on the other hand, that the presence of the blast acts to confine the plume and, initially at least, to constrain its rate of growth. Whereas in a truly steady situation the boundaries of the plume would be at atmospheric pressure, the unsteady environment due to the blast wave establishes a pressure field which decays to the atmospheric limit only asymptotically.

The flow outside the muzzle, within the plume, is source-like and has been treated by Oswatitsch as though it were a spherically symmetric expansion. Since the expansion zone is supersonic, it produces a continuously decreasing pressure field. Along the plume boundary, however, the pressure must match the conditions created behind the blast. Accordingly, the flow at the boundaries fails to be spherically symmetric; the outer streamlines are turned inwards, resulting in the formation of the lateral or barrel shock. As noted by Erdos and Del Guidice,⁵ the exterior pressure field therefore positions the boundaries of the plume, the Mach disk and the lateral or barrel shock. However, the supersonic flow within the shock system is independent of the exterior pressure field. Because the mechanical relaxation time of the part of the plume contained within the lateral shock system and the Mach disk is short by comparison with the time scale over which the muzzle conditions change, the expansion zone is approximately steady.

According to Schmidt et al.,² predictions of the Mach disk location can be performed successfully using an empirical steady state correlation, based on the instantaneous muzzle conditions.

By contrast, the region between the Mach disk and the blast front is always unsteady. Erdos and Del Guidice⁵ have shown that the centerline properties of this region, termed by them the shock layer, can be analyzed as a spherically symmetric flow with a suitably positioned center.

The foregoing discussion of the flow structure is pertinent not only to the precursor flow, but also to the propellant gas flow when the projectile has penetrated the blast region and the precursor flow has been enveloped by that due to the propellant gas.

The sketch of Figure 1.1 depicts the propellant blast field at an intermediate point when the projectile is still within the plume. At this time the Mach disk is replaced by the base shock⁵ at the projectile base. It was thought by Erdos and Del Guidice, from consideration of their data, that the base shock falls back from the projectile base to form the Mach disk when the pressure downstream of the shock accords with that which would be produced behind the Mach disk in the absence of the projectile.

Distortion of the propellant gas flow, with respect to the structure exhibited by the precursor, is due not only to the projectile, but also, of course, to the existence of the precursor flow itself. Schmidt and Shear⁴ note the delay in the formation of a strong propellant blast until the propellant gas penetrates the Mach disk of the precursor jet. Subsequently, the blast strength becomes greatest along the axis of symmetry, as expected. The air blast due to the propellant gas is found to require approximately 100 μ sec to assume a roughly spherical shape in their studies of an M-16 rifle.

Apart from differences in structure, there are differences in degree associated with the precursor and propellant blasts. Typically, the initial ratio of muzzle to ambient pressure has a value of the order of ten for the precursor and of the order of several hundred for the propellant blast. There are also differences in the ratio of specific heats, that for the propellant being lower than that for the precursor. Accordingly, the expansion angle at the muzzle is much greater for the propellant gas jet than for the precursor, as would be expected from the Prandtl-Meyer theory of steady supersonic expansion.⁸

We now comment on the occurrence of flash due to the interaction of the propellant gas with the external atmosphere. We follow the discussion given by Klingenberg⁶ and by Klingenberg et al.^{9, 10}

Three luminous regions, separated in space and time, are identified from studies of a 7.62-mm rifle. First, adjacent to the muzzle is a small region of low luminosity, referred to as the primary flash. Second, just beyond the muzzle and separated from the primary flash by a dark zone is a region of high luminosity, referred to as the intermediate flash. Third, adjacent to the intermediate flash and extending further downstream is a region of high luminosity, referred to as the secondary flash.

⁸ Liepmann, H. W. and Roshko, A.
"Elements of Gasdynamics"
John Wiley & Sons

1957

⁹ Klingenberg, G. and Mach, H.
"Investigation of Combustion Phenomena Associated with the Flow
of Hot Propellant Gases - I: Spectroscopic Temperature
Measurements Inside the Muzzle Flash of a Rifle"
Combustion and Flame, vol. 27, no. 2

October 1976

¹⁰ Klingenberg, G. and Schröder, G. A.
"Investigation of Combustion Phenomena Associated with the
Flow of Hot Propellant Gases - II: Gas Velocity Measurements
by Laser-Induced Gas Breakdown"
Combustion and Flame, vol. 27, no. 2

October 1976

The primary flash is considered to represent thermal radiation due to the elevated temperature of the propulsion gas within the Mach cone at the muzzle. The expansion fan at the muzzle produces a rapid cooling of the exhausting gas and the concomitant drop in luminosity yields a dark zone. However, as the gas is overexpanded and is therefore strongly recompressed on passing through the Mach disk, the temperature may be elevated sufficiently at that point not only to yield thermal radiation, but also to excite a significant degree of exothermic reaction. This process of shock recompression, accompanied perhaps by renewed chemical reaction of the propellant gas, is responsible for the intermediate flash. The secondary flash, when it occurs, is associated with the turbulent mixing of the hot, recompressed fuel-rich propellant gas with ambient oxygen.

Verification of the foregoing statements was made by Klingenberg and Mach⁹ on the basis of temperature measurements and, with regard to the role of the ambient air in respect to secondary flash, by firing into inert gas where secondary combustion was suppressed while the primary and intermediate flash were unaltered.

It is the secondary flash which represents a design constraint. The luminosity reveals the gun position and the energy release adds substantially to the weapon blast. Klingenberg and Mach⁹ note that the energy released by secondary combustion may be comparable to that released within the tube. In a review of the implications of blast on the design of naval weapons, Yagla¹¹ reports secondary pressures from a reduced round as high as 3.8 times the primary pressure from the full charge round.

An elementary basis for the determination of the occurrence of muzzle flash was established by Carfagno¹² and used with some success by Heiney and Powers¹³ and by May and Einstein,¹⁴ the latter

¹¹Yagla, Jon J.

"Analysis of Gun Blast Phenomena for Naval Architecture, Equipment, and Propellant Charge Design"

Third International Symposium on Ballistics

Karlsruhe, Germany

March 1977

¹²Carfagno, S. P.

"Handbook on Gun Flash"

The Franklin Institute

November 1961

¹³Heiney, O. K. and Powers, R. J.

"Secondary Muzzle Gas Combustion Considerations in Aircraft Cannon"

Proceedings of the 14th JANNAF Combustion Meeting

August 1977

¹⁴May, I. W. and Einstein, S. I.

"Prediction of Gun Muzzle Flash"

Proceedings of the 14th JANNAF Combustion Meeting

August 1977

having introduced some corrections. The method described by May and Einstein incorporates the physical picture of the secondary combustion process described in the preceding paragraphs. The method is purely one-dimensional and considers the successive thermodynamic state changes associated with isentropic expansion of the propellant gas from muzzle conditions to atmospheric pressure, shock recompression at the Mach disk, expansion to atmospheric pressure once again, and mixing with ambient air in some ratio r . The temperature of the mixture is then computed, with a suitable allowance for the fraction of the energy associated with motion of the mixture. The temperature, as a function of the mixture ratio r , is then compared with the chemical ignition limit curve. If overlap occurs, including a 100°K safety factor, ignition is predicted.

A more recent study of secondary flash has been reported by Yousefian and May¹⁵ based on a steady state analysis of the turbulent afterburning region including a detailed representation of the finite rate chemical kinetics.

We conclude by noting that some success has been achieved by several authors^{2,16,17} in respect to the determination of scaling laws for the propellant blast. Schmidt et al² exhibit quite good extrapolation of 20 mm blast data to a 7.62 mm rifle and to 75 mm and 105 mm weapons. Several attempts have been made to simulate the blast field by means of a numerical solution of the hydrodynamic equations. The recent survey by Schmidt¹⁸ may be consulted for a summary of work in this area.

¹⁵ Yousefian, V. and May, I. W.

"Prediction of Muzzle Flash Onset"

Proceedings of the 16th JANNAF Combustion Meeting

1979

¹⁶ Smith, F.

"A Theoretical Model of the Blast From Stationary and Moving Guns"

First International Symposium on Ballistics

Orlando, Florida

November 1974

¹⁷ Westine, P.

"The Blast Field About the Muzzle of Guns"

Shock and Vibration Bulletin, vol. 39, part 6

March 1969

¹⁸ Schmidt, E.

"Survey of Muzzle Blast Research"

Fifth International Symposium on Ballistics

April 1980

2.0 PROPAGATION OF SOUND

It is well known¹⁹ that Newton, in his pioneering theoretical estimate of the speed of sound in air, treated the temperature as constant with the result

$$a = \sqrt{g_0 p / \rho} \quad 2.1$$

where a is the speed of sound, p is the pressure, ρ is the density and g_0 is a constant to reconcile units of measurement. The value so calculated was found to fall short of the observed value by about 16%. It is equally well known that Laplace offered the suggestion that as the condensations and rarefactions associated with the propagation of sound take place with great rapidity, the temperature could not, in fact, be constant. Insufficient time would elapse, during each oscillation, for heat transfer to occur. Thus, the appropriate relationship between pressure and density is the adiabatic law, whereupon it is found that

$$a = \sqrt{\gamma g_0 p / \rho} \quad 2.2$$

where γ is the ratio of specific heats.

The value calculated by means of 2.2 agrees with observation, science marches on, the reasoning of Laplace is a familiar fixture in widely accepted textbooks,²⁰ and, in fact, while 2.2 is correct, the reasoning is not. It is pointed out by Liepmann and Roshko⁸ that the process is adiabatic not because the oscillations are rapid, but because they are slow enough that the induced velocity and temperature gradients are kept small. At sufficiently high frequencies the gradients do in fact increase to the point where viscous and thermal dissipation become significant and the process then tends to be isothermal rather than adiabatic.

The purpose of this preamble is not to suggest that Newton was incompetent, or that Laplace was a fraud.* We take the foregoing as a caution: Determining the speed of sound may not be as simple as we would like it to be in the present context. Where Newton and Laplace have stumbled, we had better tread with care. One's sense of caution

¹⁹

Strutt, J. W. (Baron Rayleigh)
"The Theory of Sound" Vol. II
Dover Publications

1945

²⁰

Goldstein, H.
"Classical Mechanics"
Addison-Wesley

1959

*One might however suggest that a great number of working physicists have had their minds poisoned in connection with what is generally regarded as an elementary matter.

may be heightened by an account given by Blackstock²¹ of the errors made by such luminaries as Euler, Lagrange, Poisson, Stokes and Earnshaw in connection with the theory of the propagation of finite amplitude sound.

Part of the difficulty in establishing the speed of sound is associated with the definition of sound itself. In the simplest terms we may ask how long it takes for a signal impressed on a medium at one point to travel to another where it is to be detected. If the medium is an ideal gas at rest, apart from the perturbing influence of the signal, and if the influence of the signal is such as to induce extremely small motions of the medium, then 2.2 gives the signal speed and the speed is independent of the spectral content of the signal. It does not matter whether the signal is a pure oscillation of fixed finite frequency or whether it involves a superposition of such oscillations, the total amplitude being small, or even whether the signal involves a discontinuity, again provided that the amplitude is small.

In reality, however, gases possess internal degrees of freedom which are local attributes with respect to the length scales which validate the continuum hypothesis. These degrees of freedom are associated with the vibrational and rotational motions of individual molecules and with the formation and breaking of chemical bonds among them. If the state of the gas is locally disturbed, a finite time is associated with the adjustment of each of the internal degrees of freedom to the new state. Only when the rate at which the disturbance is imposed is large by comparison with the rates of adjustment of the internal degrees of freedom can the gas be treated as though it were in thermodynamic equilibrium.

If the signal consists of an oscillation at a single frequency--in other words, a Fourier component--then as the frequency is increased to the point where its reciprocal is comparable to the characteristic relaxation time for the internal degrees of freedom, it is found that the rate of signal propagation exhibits a dependence on frequency. Accordingly, more complex signals, composed from a superposition of Fourier components, change shape as the signal propagates--the familiar phenomenon of dispersion. In particular, a signal which is initially formed as a discontinuity, and which therefore contains Fourier components of all frequencies, will be expected to change shape as it propagates.

²¹Blackstock, D. T.
"History of Nonlinear Acoustics and a Survey of Burgers' and Related Equations"
in Nonlinear Acoustics, Proceedings of a Conference at
Applied Research Laboratories, University of Texas at Austin
AD719936

For complex signals which may be viewed as a superposition of components of different frequencies which travel at different velocities, the definition of an overall propagation rate becomes ambiguous. One may say, for example, that the signal speed will be determined by the most rapidly propagating components. But in a practical situation the portion of the total signal energy invested in the fastest moving components may be too small to be detected. Accordingly, practical considerations demand a specification of the sensitivity of the detection apparatus and a definition of the spectral content of the signal.

The plan of the present chapter is as follows. We first consider the elementary wave equation and make some observations concerning the nature of its solutions. We then draw some rather general conclusions concerning the relationship between the rate of propagation of small disturbances and the characteristic surfaces of the partial differential equations which describe the behavior of the supporting medium. With these results in hand we discuss the implications for wave propagation of such real gas effects as viscosity, thermal conductivity and chemical reactivity. We conclude by discussing the influence of macroscopically nonideal phenomena with particular reference to the presence of a dispersed particulate phase.

2.1 Speed of Sound in an Ideal Fluid

The one-dimensional, unsteady motion of a fluid which is inviscid, non-heat-conducting and nonreacting is governed by following equations.⁸

$$\frac{\partial \rho}{\partial t} + u \frac{\partial \rho}{\partial x} + \rho \frac{\partial u}{\partial x} = 0 \quad 2.1.1$$

$$\frac{\partial u}{\partial t} + u \frac{\partial u}{\partial x} + \frac{g_0}{\rho} \frac{\partial p}{\partial x} = 0 \quad 2.1.2$$

$$\frac{\partial p}{\partial t} + u \frac{\partial p}{\partial x} = \frac{a^2}{g_0} \left(\frac{\partial \rho}{\partial t} + u \frac{\partial \rho}{\partial x} \right) \quad 2.1.3$$

These are, respectively, the equation of continuity, Newton's law of motion and the statement that the entropy of a given fluid particle does not change. We have used conventional nomenclature: ρ , density; u , velocity; p , pressure; and $a = \sqrt{(\partial p / \partial \rho)_s}$ is the isentropic speed of sound. Equation 2.1.3 may be used to recast 2.1.1 as

$$\frac{\partial p}{\partial t} + u \frac{\partial p}{\partial x} + \rho \frac{a^2}{g_o} \frac{\partial u}{\partial x} = 0 \quad 2.1.4$$

Now let us write $p = p_o + p_1$ and similarly for u and ρ with the understanding that p_o, u_o, ρ_o form a solution of the equations and furthermore that p_1, u_1, ρ_1 are small quantities, so that when we substitute p, u, ρ into 2.1.2 and 2.1.4, we may neglect the squares of the quantities with subscript 1. We find that p_1 and u_1 satisfy

$$\frac{\partial p_1}{\partial t} + u_o \frac{\partial p_1}{\partial x} + \rho_o \frac{a_o^2}{g_o} \frac{\partial u_1}{\partial x} = -u_1 \frac{\partial p_o}{\partial x} - \frac{\rho_1 a_o^2 + 2\rho_o a_o a_1}{g_o} \frac{\partial u_o}{\partial x} \quad 2.1.5$$

$$\frac{\partial u_1}{\partial t} + u_o \frac{\partial u_1}{\partial x} + \frac{g_o}{\rho_o} \frac{\partial p_1}{\partial x} = -u_1 \frac{\partial u_o}{\partial x} + \frac{g_o \rho_1}{\rho_o^2} \frac{\partial p_o}{\partial x} \quad 2.1.6$$

We could similarly linearize 2.1.3 to determine an additional equation for ρ_1 , but this is irrelevant to our present purpose.

Now let the state designated by subscript o be quiescent and uniform. Evidently, 2.1.5 and 2.1.6 reduce to

$$\frac{\partial p_1}{\partial t} + \frac{\rho_o a_o^2}{g_o} \frac{\partial u_1}{\partial x} = 0 \quad 2.1.7$$

$$\frac{\partial u_1}{\partial t} + \frac{g_o}{\rho_o} \frac{\partial p_1}{\partial x} = 0 \quad 2.1.8$$

Then differentiating 2.1.7 with respect to x and 2.1.8 with respect to t and eliminating $\partial^2 p_1 / \partial x \partial t$, we have the familiar wave equation

$$\frac{\partial^2 u_1}{\partial t^2} = a_o^2 \frac{\partial^2 u_1}{\partial x^2} \quad 2.1.9$$

Since this is a linear equation, we can suppose u_1 to be a sum of Fourier components, each of which is a solution of 2.1.9. If

$$\phi = \phi(\omega) e^{i(kx - \omega t)} \quad 2.1.10$$

is such a component, then, evidently

$$k = \pm \omega / a_o \quad 2.1.11$$

and the amplitude $\phi(\omega)$ is determined by other considerations, namely, the initial and boundary data which serve to single out particular solutions of 2.1.9.

Now the rate of propagation of each component is evidently $\text{Re}(k/\omega) = \pm a_0$ and the rate of attenuation is given by $\text{Im}(k/\omega) = 0$ in the present case. Therefore, the motion described by 2.1.9 is such that each Fourier component propagates with constant velocity, to the left or the right according as $k = -\omega/a_0$ or $+\omega/a_0$, respectively, and without change in amplitude. As a corollary, a complex signal formed as a linear superposition of Fourier components also propagates with constant velocity.

Using 2.1.11, let us write the pair of solutions of the type 2.1.10 in the form

$$\phi_{\pm} = \phi_{\pm}(\omega) e^{\pm \frac{i\omega}{a_0}(x \mp a_0 t)} \quad 2.1.12$$

Evidently, 2.1.12 implies that on lines of the form

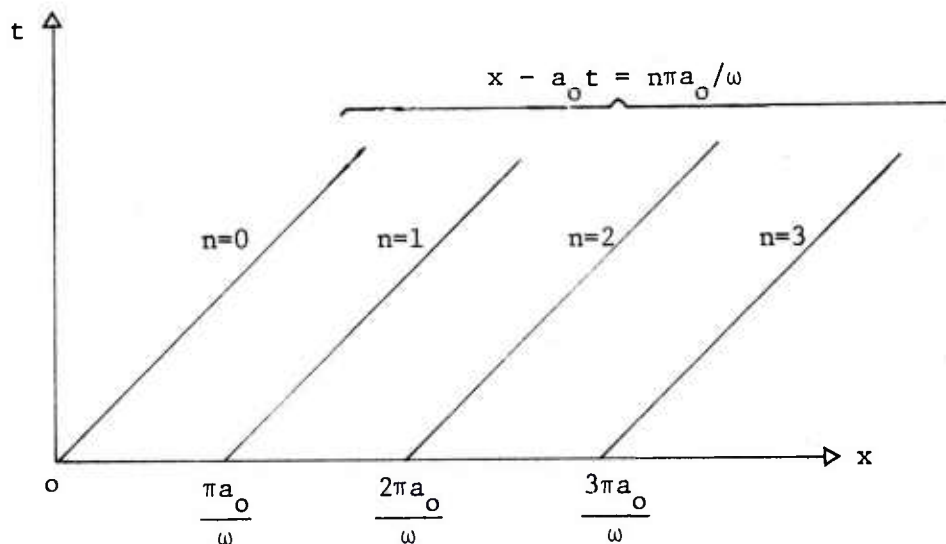
$$x \pm a_0 t = \ell_{\pm} \quad 2.1.13$$

where x_0 is a constant, we have the property

$$\phi_{\pm} = \phi_{\pm} e^{\pm \frac{i\omega}{a_0} \ell_{\pm}} \quad 2.1.14$$

so that the solution is constant.

Now consider the family of lines of the type defined by 2.1.13 with $\ell_{+} = n\pi a_0/\omega$, $n = 0, 1, 2, \dots$, as shown in the sketch below.



On each such line we have $\phi_+ = \phi_+ e^{in\pi} = \phi_+ (-1)^n$ so that ϕ_+ clearly alternates between the extreme values $\pm\phi_+$ as we pass from one member of the family to the next. Suppose now that we let $\omega \rightarrow \infty$. It follows that the rate of variation of ϕ_+ in the direction normal to each of the members of the family becomes unboundedly large. The normal spacing between the members goes to zero while the value of ϕ_+ continues to alternate between the extremes $\pm\phi_+$.

From a physical point of view we may identify these lines with the paths followed by infinitesimal disturbances of the fluid. But from a mathematical point of view we see that they have the interesting property that certain members of the solution space always have a vanishing derivative along them while the same members may have an unbounded derivative in the direction normal to them. This property is a reflection of the possibility that lines of the type 2.1.13 may separate regions of the $x - t$ plane in which the solution u has different analytical properties so that either u or its derivatives above some order suffers a discontinuous jump as we pass from one region to another.

For example, we may suppose that u initially is equal to 1 everywhere in the left half-plane and 0 everywhere in the right half-plane. Evidently the solution will remain equal to 1 for $x < -a_0 t$ and will remain equal to 0 for $x > a_0 t$ since, from a physical perspective, these inequalities define the time delay for information from one half-plane to affect the other.

The importance of the lines defined by 2.1.13 is further emphasized if we transform the independent variables x and t into the pair ℓ_+ and ℓ_- . Equation 2.1.9 becomes

$$\frac{\partial^2 u_1}{\partial \ell_+ \partial \ell_-} = 0 \quad 2.1.15$$

so that the general solution of 2.1.9 is therefore

$$u_1(x, t) = F(x - a_0 t) + G(x + a_0 t) \quad 2.1.16$$

which is the form attributed to D'Alembert. Since 2.1.16 follows without reference to a Fourier decomposition, it follows immediately that the signal propagation speed is $\pm a_0$ independently of its frequency.

2.2 Characteristic Lines

In the preceding section we determined the speed of sound by looking at the rate of propagation of a single Fourier component whose amplitude was sufficiently small as to justify the linearization of the governing equations for an ideal fluid. We also assumed that the unperturbed state was quiescent and uniform, a point to which we shall return subsequently.

We noted that the lines along which sound impulses travel hold the potential for separating two regions of different analytical character. This suggests an alternative approach to the definition of signal speed. We may ask whether the balance equations admit the existence of real lines across which the derivatives of the state variables may jump discontinuously. The advantage of posing the question in this form is that no assumptions need be made about the uniformity of the flow. The existence of the lines, or otherwise, is a property of the nonlinear balance equations. No reference is made to the spectral content of the signal associated with such lines, nor is the ultimate change of state induced by the signal necessarily to be regarded as small.

There are many ways of formulating this question mathematically. Shapiro²² considers the determinacy of the x and t derivatives when the solution is known on a given line of slope dx/dt . Courant and Friedrichs²³ pose the question in terms of the directions in which the state variables are differentiated. Although it entails greater generality than we actually need here, we follow the approach of Petrovsky²⁴ since it is actually the most illuminating in a fundamental sense.

Consider the quasilinear system of partial differential equations

$$\sum_{j,k_0,k_1,\dots,k_n} A_{ij}^{(k_0,\dots,k_n)} \frac{\partial^{n_j} y_j}{\partial x_0^{k_0} \partial x_1^{k_1} \dots \partial x_n^{k_n}} + \dots + f_i = 0 \quad 2.2.1$$

²²Shapiro, A. H.

"The Dynamics and Thermodynamics of Compressible Fluid Flow"
Ronald Press

1953

²³Courant, R. and Friedrichs, K. O.

"Supersonic Flow and Shock Waves"
Interscience

1948

²⁴Petrovsky, I. G.

"Partial Differential Equations"
Interscience

1954

where $i, j = 1, 2, \dots, N$. Thus, we have N equations, labelled by the subscript i , involving N dependent variables y_j and $n + 1$ independent variables x_0, \dots, x_n . In each equation we only write explicitly the highest order terms for each y_j that appears in the system as a whole. This maximum order is designated by n_j for each variable y_j .

Now consider an arbitrary surface whose intrinsic coordinates are ξ_1, \dots, ξ_n and let ξ_0 be a coordinate in a direction normal to the surface. We assume that we have Cauchy data on this surface, namely, the values of the y_j and all their derivatives of order less than n_j . Then the surface is said to be free if the system 2.2.1 enables the determination of the $\partial^{n_j} y_j / \partial \xi_0^{n_j}$, $j = 1, \dots, N$ and characteristic if it does not.

It follows from an application of the point transformation $\{x_i\} \rightarrow \{\xi_i\}$ that the values of the $\partial^{n_j} y_j / \partial \xi_0^{n_j}$ are the solution of a linear algebraic system of equations whose matrix of coefficients is

$$\{\Delta_{ij}\} = \left\{ \sum_{k_0 + k_1 + \dots + k_n = n_j} A_{ij}^{(k_0, \dots, k_n)} \mu_0^{k_0} \mu_1^{k_1} \dots \mu_n^{k_n} \right\} \quad 2.2.2$$

where $\mu_i = \partial \xi_0 / \partial x_i$, $i = 0, 1, \dots, n$. The μ_i may be interpreted as the components of a vector normal to the surface $\xi_0 = \text{constant}$. Then the given surface is evidently characteristic if and only if the rank of Δ_{ij} is less than N .

For a first order system like 2.1.1, 2.1.2, 2.1.3 we may take $x_0 = t$ and $x_1 = x$ so that the system may be expressed in the form

$$A_{ij} \frac{\partial y_j}{\partial t} + B_{ij} \frac{\partial y_j}{\partial x} = C_i \quad 2.2.3$$

whence

$$\Delta_{ij} = \mu_t A_{ij} + \mu_x B_{ij} \quad 2.2.4$$

and we have the slope of the characteristic lines in the form

$$\frac{dx}{dt} = - \frac{\mu_t}{\mu_x} \quad 2.2.5$$

In the previous section we determined the rate of propagation of small disturbances by reference to equations 2.1.2 and 2.1.4. In principle we should evaluate the characteristic matrix for the complete set 2.1.1, 2.1.2 and 2.1.3. For the sake of comparison with the preceding section, however, we consider only 2.1.2 and 2.1.4 in the present section also. The effect of including 2.1.3 is simply to establish the fluid streamline as a characteristic along which the entropy of the fluid is conserved.

Using 2.1.2 and 2.1.4 with $y_1 = p$ and $y_2 = u$ in 2.2.3, we see that

$$\Delta = \begin{bmatrix} \mu_t + u\mu_x & \rho \frac{a^2}{g_o} \mu_x \\ \mu_x \frac{g_o}{\rho} & \mu_t + u\mu_x \end{bmatrix} \quad 2.2.6$$

The rank of Δ will be less than 2 if $\det(\Delta) = 0$ or

$$(\mu_t + u\mu_x)^2 - a^2 \mu_x^2 = 0 \quad 2.2.7$$

Thus, using 2.2.5, we have the slope of the characteristic lines

$$\frac{dx}{dt} = u \pm a \quad 2.2.8$$

The relationship of this result to 2.1.13 is obvious and, from the discussion of the previous section, not unexpected. Also, in the previous section we noted the invariance of certain quantities along the acoustic paths. The corresponding generalization may be found in the present context from the observation that the derivatives normal to the characteristic surface are not infinite, merely undetermined by the equations and the Cauchy data. Then the condition of solvability yields a constraint on the Cauchy data which is usually referred to as the condition of compatibility. Since we are only concerned with the characteristics themselves, we do not derive the corresponding conditions of compatibility.

While 2.2.8 seems naturally related to 2.1.13, we should observe that it is not simply the extension of 2.1.13 to account for a non-quiescent, nonuniform flow. To understand this point more clearly, let us use 2.1.5 and 2.1.6 rather than 2.1.9 as we did previously. For the sake of simplicity we assume that the fluid is isentropic and obeys the ideal gas law so that we may write $\rho_1 = g_o p_1 / a_o^2$

and $a_1 = (\gamma - 1)g_0 p_1 / (2a_0 \rho_0)$. Analogously with 2.1.10 we put $p_1 = \bar{p}_1 e^{i(kx - \omega t)}$ and $u_1 = \bar{u}_1 e^{i(kx - \omega t)}$. Substituting in 2.1.5, 2.1.6 we obtain two homogeneous linear equations for \bar{p}_1 and \bar{u}_1 . The condition that a nontrivial solution exists is

$$\det \begin{bmatrix} -\omega + ku_0 - i\gamma \frac{\partial u_0}{\partial x} & \frac{\rho_0 a_0^2}{g_0} k - i \frac{\partial p_0}{\partial x} \\ \frac{g_0}{\rho_0} k + i \left(\frac{g_0}{\rho_0 a_0} \right)^2 \frac{\partial p_0}{\partial x} & -\omega + ku_0 - i \frac{\partial u_0}{\partial x} \end{bmatrix} = 0 \quad 2.2.9$$

Evidently, when the unperturbed flow is uniform, 2.2.9 is formally identical with 2.2.6 if we let $\mu_t \rightarrow -\omega$ and $\mu_x \rightarrow k$. In general, however, when the unperturbed flow is nonuniform, 2.2.9 corresponds with 2.2.6 only in the limit as $\omega, k \rightarrow \infty$. Thus, the characteristic lines correspond to the paths followed by high frequency signals. Equation 2.2.9 may be recast as

$$\begin{aligned} & [-\omega + ku_0 (1 - \frac{i\gamma}{ku_0} \frac{\partial u_0}{\partial x})] [-\omega + ku_0 (1 - \frac{i}{ku_0} \frac{\partial u_0}{\partial x})] \\ & = k^2 a_0^2 [1 + (\frac{\partial p_0 / \partial x}{\gamma p_0 k})^2] \end{aligned} \quad 2.2.10$$

An examination of 2.2.10 makes the definition of high frequency more precise. We require the wavelength to be small by comparison with the length scale over which significant changes can occur in the unperturbed fluid.

Whereas the rate of propagation of a Fourier component was found to be independent of frequency for a uniform, quiescent state, 2.2.10 shows the wave velocity to be dispersive in the more general case.

It is of interest to compare the finite frequency wave speed with the limiting characteristic value. For simplicity assume $u_0 = 0$ in 2.2.10, so that we consider only the influence of $\partial p_0 / \partial x \neq 0$. Evidently, for finite k ,

$$\frac{\omega}{k} = \pm a_0 \left[1 + \left(\frac{\partial p_0 / \partial x}{\gamma p_0 k} \right)^2 \right]^{1/2} \quad 2.2.11$$

so that the velocity of a monochromatic wave is greater than $a_0 = \lim_{k \rightarrow \infty} (\omega/k)$. However, the group velocity for a signal with dominant wave number k is given by the formula²⁵

$$V_g = \frac{d\omega}{dk} = \pm a_0 \left[1 + \left(\frac{\partial p_0 / \partial x}{\gamma p_0 k} \right)^2 \right]^{-1/2} \quad 2.2.12$$

and is always less than a_0 for finite k .

The fact that the finite frequency group velocity is less than the limiting or characteristic value in this particular case is something which one might anticipate in general from the following reasoning. Suppose the governing equations are such that they have real characteristic lines. If we now consider a process in which a localized signal is suddenly imposed on the flow--as a boundary value, for example--then we expect the signal to propagate through the medium in such a fashion that it always remains localized. Therefore, the boundary of the signal will describe a path on one side of which is undisturbed fluid and on the other side of which the fluid is disturbed in some degree. But such a line is precisely a characteristic line since it admits a change in analytic properties from one side to the other. Accordingly, we expect the characteristic lines to represent the maximum propagation rates of localized signals--independently of the underlying dispersive mechanisms. By its very nature a single monochromatic wave cannot represent a localized signal--it extends throughout all space. Accordingly, the fact that the phase velocity 2.2.11 exceeds a_0 in general is not a cause for concern. The relevant quantity in respect to the propagation of a wave packet is the group velocity which, as we have seen in 2.2.12 in particular, is always expected to be less than a_0 .

The physical significance of the group velocity as the rate of propagation of a wave packet or isolated polychromatic signal is emphasized not only in problems of sound transmission through a gas but also in problems of structural mechanics²⁶ and electrodynamics.²⁷

²⁵ Landau, L. D. and Lifshitz, E. M.
"Fluid Mechanics"

Pergamon Press 1959

²⁶ Fung, Y. C.

"Foundations of Solid Mechanics"

Prentice-Hall 1965

²⁷ Jackson, J. D.

"Classical Electrodynamics"

John Wiley and Sons 1962

Equation 2.2.9 has been shown to yield a wave velocity for a single Fourier component which becomes equal to the characteristic wave speed in the limit of very high frequencies. Since $\lim_{\omega \rightarrow \infty} (\omega/k)$

exists it follows by L'Hospital's rule that $\lim_{\omega \rightarrow \infty} \left(\frac{\omega}{k}\right) = \lim_{\omega \rightarrow \infty} \left(\frac{d\omega}{dk}\right)$.

Thus, the group velocity will also tend to the characteristic value in the limit of high frequencies. We could have seen this from 2.2.12, of course, but the present argument does not require $u_0 = 0$ as was assumed in the derivation of 2.2.12.

The equality of the high frequency monochromatic wave speed and the characteristic wave speed is a result of very general validity and is not confined to the particular example we have been considering here. Proofs of the equality for the case of systems of quasi-linear partial differential equations with two independent variables have been given by Gough²⁸ and by Ramshaw and Trapp.²⁹

2.3 Speed of Sound in Real Gases

The preceding sections have shown that signal propagation in an ideal fluid can be given an unequivocal meaning if the fluid is initially uniform and at rest and if the strength of the signal does not appreciably affect the equilibrium of the fluid. Dispersion, or a dependence of wave speed on frequency, arises when the flow is non-uniform and therefore when the fluid departs significantly from an equilibrium state during the passage of a signal. In the event of significant departures from equilibrium, an unequivocal definition of signal speed can still be established in terms of the high frequency limit for monochromatic waves which is also the speed of propagation of discontinuities of the derivatives of the state variables. For signals which have a finite frequency content which is clustered about some dominant value, the propagation rate may be defined as the group velocity which is not expected to exceed the high frequency wave speed.

In real gases dispersion arises when the initial condition is uniform and quiescent and the amplitude of the signal is small. In section 2.3.1 we will consider the effects of viscosity and thermal conductivity, and in 2.3.2 we will consider the influence of departures from equilibrium of the internal degrees of freedom with particular reference to the finite rates of reaction of a mixture of gases.

²⁸ Gough, P. S.

"Fundamental Investigation of the Interior Ballistics of Guns"
Naval Ordnance Station, Indian Head, MD
IHCR 74-1

1974

²⁹ Ramshaw, J. D. and Trapp, J. A.

"Characteristics, Stability and Short-Wavelength Phenomena
in Two-Phase Flow Equation Systems"
ANCR-1272

1976

We consider only gases. The dispersive mechanisms particular to condensed phases are discussed in References 30 and 31, to name two examples. Also, because our interest is confined to an unloading wave, we do not consider the processes associated with finite waves of discontinuity, namely, shock waves. We do note, however, that due to the fact that shocks involve finite changes of state over a period of time comparable to the mean free time between molecular collisions, departures from thermodynamic equilibrium can be considerable. Studies of the structure of shock waves therefore provide a useful means of determining the internal relaxation times of both inert and reacting gases.³²

2.3.1 Effects of Viscosity and Thermal Conductivity

To consider the effects of viscosity we must extend the mechanical constitutive law so as to recognize that the force exerted on a fluid element by its neighbors is represented by a tensor σ_{ij} rather than the scalar p . Then, using p to denote the pressure given by the equilibrium equation of state based on the instantaneous density and temperature, we have^{25,26,30}

$$\sigma_{ij} = (-p + \lambda \frac{\partial u_k}{\partial x_k}) \delta_{ij} + \mu (\frac{\partial u_i}{\partial x_j} + \frac{\partial u_j}{\partial x_i}) \quad 2.3.1$$

Here we have used μ and λ to represent the first and second coefficients of viscosity, δ_{ij} is the Kronecker delta, u_i is a velocity component and x_i is the corresponding Cartesian coordinate. The repeated index indicates a sum. In accordance with the conventions of continuum mechanics, the tensile stress is taken to be positive. The coefficient μ defines the resistance of the fluid to deformation, and 2.3.1 asserts that the shear stress is proportional to the deformation rate. The effective pressure is given by

$$p_{\text{eff}} = -\frac{1}{3} \sigma_{kk} = p - (\lambda + \frac{2\mu}{3}) \frac{\partial u_k}{\partial x_k} \quad 2.3.2$$

³⁰Malecki, I.

"Physical Foundations of Technical Acoustics"
Pergamon Press

1969

³¹Hueter, T. F. and Bolt, R. H.
"Sonics"

John Wiley and Sons, NY

1955

³²Greene, E. F. and Toennies, J. P.
"Chemical Reactions in Shock Waves"
Academic Press

1964

According to Stokes' hypothesis, no friction is associated with a pure dilatation so that $p_{\text{eff}} = p$ and therefore

$$\mu' = \lambda + \frac{2\mu}{3} = 0 \quad 2.3.3$$

Sometimes the quantity μ' rather than λ is referred to as the second coefficient of viscosity.³³ In general μ' is not zero. However, a nonzero value of μ' is associated with a finite rate of equilibration of the internal degrees of freedom and may therefore be regarded as part of the discussion of the next section. If 2.3.3 is used in 2.3.1, we have

$$\sigma_{ij} = - \left(p + \frac{2\mu}{3} \frac{\partial u_k}{\partial x_k} \right) \delta_{ij} + \mu \left(\frac{\partial u_i}{\partial x_j} + \frac{\partial u_j}{\partial x_i} \right) \quad 2.3.4$$

The use of this constitutive law leads to the following equation for the one-dimensional propagation of small amplitude disturbances through an initially quiescent and uniform gas³⁰

$$\frac{\partial^2 u}{\partial t^2} = a_0^2 \frac{\partial^2 u}{\partial x^2} + \frac{4}{3} \frac{\mu}{\rho} \frac{\partial^2 u}{\partial x \partial t} \quad 2.3.5$$

which may be compared with the inviscid result 2.1.9. The substitution of a monochromatic Fourier component $e^{i(kx - \omega t)}$ yields³⁰

$$\text{Re} \left(\frac{\omega}{k} \right) = a_0 \left\{ \frac{2[1 + Q^2]}{(1 + Q^2)^{1/2} + 1} \right\}^{1/2} \quad 2.3.6$$

as the phase velocity where

$$Q = \frac{4}{3} \frac{\mu}{\rho} \frac{\omega}{a_0^2} \quad 2.3.7$$

Since the phase velocity depends on ω through Q , the medium is dispersive. Moreover, $\lim_{\omega \rightarrow \infty} \text{Re}(\omega/k) = \infty$ so that the representation of the influence of viscosity by means of 2.3.4 yields signal speeds which are infinite in the limit of high frequencies. The corresponding

³³ Zeldovitch, Ya. B., and Raizer, Yu. P.
 "Physics of Shock Waves and High Temperature Hydrodynamic Phenomena"
 Academic Press

characteristic equation is easily seen to be $dx/dt = \infty$. This follows by replacing $\frac{\partial p}{\partial x}$ by $\frac{\partial p}{\partial x} - \frac{4}{3} \mu \frac{\partial^2 u}{\partial x^2}$ in equation 2.1.2 and applying 2.2.2 to 2.1.2 and 2.1.4.

This analytical detail is of no physical significance. Equation 2.3.6 shows that significant dispersion due to viscosity occurs when $Q \approx 1$. But if we recall the following approximate relationship between the viscosity μ and the mean free path λ ³⁴

$$\mu \sim \frac{1}{3} \rho a_o \lambda \quad 2.3.8$$

then 2.3.7 shows that a value of $Q = 1$ corresponds to

$$\omega \sim a_o / \lambda \quad 2.3.9$$

Thus significant dispersion is associated with wavelengths of the order of the mean free path and with frequencies equal to the collision frequency. These conditions represent boundaries on the regime of validity of the continuum equations, and the inviscid propagation rates may be thought of as correct to within wavelengths one order of magnitude greater than the mean free path.

Apart from the bounds on the regime of physical applicability, we should observe that the mathematical formulation behaves in a reasonably well posed manner due to the influence of the rate of damping of the high frequency components. We find³⁰

$$\text{Im}(k) = \left\{ \frac{\omega}{a_o} \frac{(1 + Q^2)^{1/2} - 1}{2(1 + Q^2)} \right\}^{1/2} \quad 2.3.10$$

Thus, the damping per unit length becomes $\sqrt{3\rho\omega/4\mu}$ in the high frequency limit. While high frequency components of a mathematical solution will propagate at rates which are physically unattainable, they are at the same time sharply damped so that their quantitative influence will be negligible.

The effect of thermal conductivity is somewhat different. If k_c is the coefficient of thermal conductivity, then equation 2.1.3 must be modified as follows

³⁴ Sears, F. W.

"Thermodynamics, The Kinetic Theory of Gases, and Statistical Mechanics"
Addison-Wesley 2nd Ed.

1959

$$\left(\frac{\partial p}{\partial t} + u \frac{\partial p}{\partial x}\right) = \frac{a_o^2}{g_o} \left(\frac{\partial p}{\partial t} + u \frac{\partial p}{\partial x}\right) + \frac{k_c}{\gamma - 1} \frac{\partial^2 T}{\partial x^2} \quad 2.3.11$$

where T is the temperature. If we then consider the perturbation of ρ , u , p about a quiescent uniform state, using equations 2.1.1, 2.1.2 and 2.3.11, and assume that ρ , p , T are connected by an ideal gas law, the following dispersion equation is found

$$k^4 - k^2 \left(\frac{\omega^2}{a_o^2/\gamma} + \frac{i\omega}{\theta} \right) + \frac{i\omega^3}{a_o^2\theta} = 0 \quad 2.3.12$$

where $\theta = k_c/\rho C_p$ and C_p is the specific heat at constant pressure. This equation is fourth order and describes both the acoustic wave and an associated thermal wave driven by the induced temperature gradient. The root associated with the thermal wave has a phase velocity which behaves like $\sqrt{\omega}$ and is accordingly unbounded as $\omega \rightarrow \infty$. This property of 2.3.11 is also seen, of course, from a characteristic analysis. As with the viscous wave, the rate of damping increases with ω and the discussion of the high frequency behavior from a mathematical point of view is as given previously in connection with the effect of viscosity.

The behavior of the acoustic root is discussed by Landau and Lifshitz.²⁵ In the limit of small frequencies $\omega \ll a_o^2/\theta$ we find $\text{Re}(\omega/k) \rightarrow a_o$ as expected. It is noted that during one period heat is transmitted through a distance $\sim \sqrt{\theta/\omega}$ which is small compared with the wavelength a_o/ω , in this limit. On the other hand, at high frequencies $\text{Re}(\omega/k) \rightarrow a_o/\sqrt{\gamma}$ which is the isothermal velocity proposed by Newton. This observation should clarify the comments of Liepmann and Roshko which we quoted in the preamble to this chapter.

The condition $\omega \sim a_o^2/\theta$ can easily be seen to be equivalent to $\omega \sim a_o/\lambda$, by using 2.3.8 and assuming the Prandtl number $\mu C_p/k_c \sim 1$. Thus, the effects of both viscosity and thermal conductivity may be neglected in respect to the rate of propagation of Fourier components whose wavelength is at least one order of magnitude greater than the mean free path.

2.3.2 Effects of Finite Molecular Relaxation Times

We consider now the influence on the speed sound of the finite rates of equilibration of the internal degrees of freedom of the gas. By the expression internal degrees of freedom we refer not only to the translational, rotational and vibrational motions of individual molecules, but also to their relative number densities, that is to say,

the composition of the gas if more than one species is present. These finite rates of equilibration are intimately connected with the second viscosity coefficient in equation 2.3.1. The influence of the internal degrees of freedom can be analyzed in a general form according to the method of Mandelshtam and Leontovich as described by Landau and Lifshitz.²⁵ We summarize the method in section 2.3.2.1. In section 2.3.2.2 we discuss the relaxation times associated with the translational, rotational and vibrational degrees of freedom of individual molecules. Then in section 2.3.2.3 we discuss the form of the relaxation time associated with chemical reactions, deducing the general fashion in which the relaxation time depends upon the reaction rate coefficients and the concentrations of the species.

2.3.2.1 The Mandelshtam-Leontovich Theory of Molecular Relaxation Phenomena

We take ξ to be a state variable with equilibrium value ξ_0 . Near equilibrium, to first order, we may suppose that changes in ξ are governed by an equation of the form

$$\dot{\xi} = -(\xi - \xi_0)/\tau \quad 2.3.13$$

where τ , a positive constant, is the relaxation time for the processes which establish the equilibrium value ξ_0 .

Close to a state of thermodynamic equilibrium we may treat the entropy as constant since the perturbations will induce changes in entropy proportional to the squares of the perturbations. Then we may view the state as characterized by the density ρ and the additional variable ξ . We suppose that all quantities have the time dependence $e^{-i\omega t}$ with suitable complex amplitudes which are fixed locally. Not only ρ and ξ , but also the equilibrium value ξ_0 must be considered as varying in time. If ξ_{00} is the value of ξ_0 in the unperturbed state, we may write $\xi = \xi_{00} + \xi'$ and $\xi_0 = \xi_{00} + \xi'_0$. Then from 2.3.13 we have

$$\xi' = \frac{\xi'_0}{1 - i\omega\tau} \quad 2.3.14$$

We view the pressure as a function of ρ and ξ so that

$$\frac{\partial p}{\partial \rho} = \left(\frac{\partial p}{\partial \rho}\right)_{\xi} + \left(\frac{\partial p}{\partial \xi}\right)_{\rho} \frac{\partial \xi}{\partial \rho} \quad 2.3.15$$

which, in view of 2.3.14, implies

$$\frac{\partial p}{\partial \rho} = \frac{1}{1 - i\omega\tau} \left\{ \left(\frac{\partial p}{\partial \rho} \right)_{\xi} + \left(\frac{\partial p}{\partial \xi} \right)_{\rho} \frac{\partial \xi}{\partial \rho} - i\omega\tau \left(\frac{\partial p}{\partial \rho} \right)_{\xi} \right\} \quad 2.3.16$$

But the sum of the first two terms within the braces on the right-hand side may be identified as the derivative of p with respect to ρ along a path of equilibrium of ξ . Thus, we write 2.3.16 in the form

$$g_0 \frac{\partial p}{\partial \rho} = \frac{1}{1 - i\omega\tau} (a_e^2 - i\omega\tau a_f^2) \quad 2.3.17$$

where a_e is the equilibrium value of $[g_0 \partial p / \partial \rho]^{1/2}$ and $a_f = [g_0 (\partial p / \partial \rho)_{\xi}]^{1/2}$ is the frozen value in which ξ is held constant.

Equation 2.3.17, which applies to a fixed element of fluid, may be viewed as the generalization of 2.1.3 to account for the failure of ξ to remain in thermodynamic equilibrium. Then equations 2.1.9 and 2.1.11 retain their validity provided we replace a_0 by $(g_0 \partial p / \partial \rho)^{1/2}$ according to equation 2.3.17. Therefore, the nonequilibrium dispersion law is given by

$$k = \omega [(1 - i\omega\tau) / (a_e^2 - i\omega\tau a_f^2)]^{1/2} \quad 2.3.18$$

When $\omega\tau \ll 1$, that is to say when the period of oscillation of the wave is long by comparison with the relaxation time, we have the approximate result²⁵

$$k = \frac{\omega}{a_e} + \frac{i\omega^2\tau}{2a_e^3} (a_f^2 - a_e^2) \quad 2.3.19$$

As expected, the phase velocity $\text{Re}(\omega/k) = a_e$, the equilibrium sound speed. Moreover, the nonzero imaginary part of k indicates the presence of damping or attenuation of the wave.

For very high frequency waves such that $\omega\tau \gg 1$, we have the approximate result²⁵

$$k = \frac{\omega}{a_f} + i \frac{a_f^2 - a_e^2}{2\tau a_f^3} \quad 2.3.20$$

Thus, the high frequency wave speed is a_f , the frozen value. The imaginary part of k is independent of ω in the high frequency limit. Comparing with 2.3.19, we see that the attenuation per unit length increases with ω , reaching the asymptotic value given by 2.3.20. According to Landau and Lifshitz²⁵ the increase is monotonic. It is also noted that $a_f > a_e$ on account of LeChatelier's principle and also because of the connection between the second viscosity coefficient λ and the difference $a_f^2 - a_e^2$, namely,

$$\lambda = \frac{\tau_p}{1 - i\omega\tau} (a_f^2 - a_e^2) \quad 2.3.21$$

The foregoing discussion has addressed the influence of a single internal degree of freedom. The generalization to many degrees of freedom is straightforward.²⁵

2.3.2.2 Translational, Rotational and Vibrational Relaxation Times

We now turn to more specific details of the internal degrees of freedom, following the discussion of Zeldovitch and Raizer.³³

Equilibrium is established most quickly for the translational degrees of freedom. Only a few collisions are required to establish a Maxwellian velocity distribution. The relaxation time for the translational degrees of freedom is of the order of the mean free time which has the value $\tau_{trans} \sim 10^{-10}$ sec for air at standard conditions.

The rotational modes of molecules are also quite rapidly equilibrated as is shown in the following table.

Rotational Relaxation of Molecules³³

Molecule	Temperature (°K)	τ_{rot} at 1 atm (sec)	Number of Collisions (-)
H ₂	300	2.1×10^{-8}	300
D ₂	288	1.5×10^{-8}	160
N ₂	300	1.2×10^{-9}	9
O ₂	314	2.2×10^{-9}	12
NH ₃	293	8.1×10^{-10}	10
CO ₂	305	2.3×10^{-9}	16

We see that in the regime of interest in the present study it will be reasonable to assume that both translational and rotational equilibrium are always maintained.

Vibrational relaxation is in general a slower process, requiring a large number of collisions as shown in the following table. Extrapolation of these data to other densities may be performed by noting

Vibrational Relaxation of Oxygen and Nitrogen ³³		
T (°K)	τ_{vib}^* (sec)	Number of Collisions (-)
Oxygen		
900	96×10^{-7}	1×10^5
1200	41×10^{-7}	5×10^4
1800	9.5×10^{-7}	1.4×10^4
2400	2.7×10^{-7}	4.5×10^3
3000	0.83×10^{-7}	1.6×10^3
Nitrogen		
3000	2.1×10^{-6}	4.6×10^4
4000	0.67×10^{-6}	1.8×10^4
5000	0.27×10^{-6}	0.8×10^4
* τ_{vib} normalized to density $n = 2.67 \times 10^{19} \text{ cm}^{-3}$		

that the value of τ_{vib} is proportional to τ_{col} the collision time which depends inversely on density. In general the value of τ_{vib} varies with temperature according to the law $\tau_{\text{vib}} \sim T^{-1/3}$, a result predicted theoretically by Landau and Teller.³³ Other molecules may relax more slowly. Green and Toennies³² report the value $\tau_{\text{vib}} = 550 \mu\text{sec}$ for carbon monoxide at 1470°K and 1 atmosphere. They comment that this is the longest value known for any molecule. Carbon dioxide also shows significant dispersion at a frequency of 15 khz due to vibrational relaxation.³¹ This frequency corresponds to a value $\tau_{\text{vib}} = 400 \mu\text{sec}$ at standard atmospheric conditions.

It should be noted that extrapolation of vibrational relaxation times of a given species of molecule into the gun environment must take into account the fact that small traces of different molecules can significantly reduce the number of collisions required to effect equilibration. The following data indicate the influence of various added gases at 1 per cent molar concentration.

Average Number of Collisions for Transfer of One Energy Quantum ³¹			
Added Gas	Primary Gas		
	Cl ₂	N ₂ O	CO ₂
None	34000	7500	50000
A	32000	-	47000
He	900	1000	2600
H ₂	780	650	300
CO	230	600	-
CH ₄	190	840	2400
NH ₃	-	450	-
HCl	120	-	130
H ₂ O	-	105	40

2.3.2.3 Chemical Relaxation Times

We may consider a general chemical reaction involving n species M_i as follows



where the v_i' are the stoichiometric coefficients for the reactants in the forward direction and for the products in the reverse direction and conversely for the v_i'' . Let C_i be the molar concentration of M_i and let k_f , k_b be the rate coefficients, functions of temperature, for the forward and backward reactions. From the law of mass action³⁵ we may

³⁵Williams, F. A.
"Combustion Theory"
Addison-Wesley

determine the net rate of change of C_j as

$$\frac{d}{dt}C_j = (v_j'' - v_j') \left\{ k_f \prod_{i=1}^n C_i^{v_i'} - k_b \prod_{i=1}^n C_i^{v_i''} \right\} \quad j=1, \dots, n \quad 2.3.23$$

We now suppose the system to be initially in equilibrium and to be perturbed in the sense of the Mandelshtam-Leontovich theory. Let C_{je} be the equilibrium values of the concentrations at each step of the perturbation. In general, due to the finite time required for the reaction to proceed, the actual values will differ from C_{je} . We put

$$C_j = C_{je} + \xi_j \quad j = 1, \dots, n \quad 2.3.24$$

where ξ_j is understood to be small by comparison with C_{je} . Substituting 2.3.24 into 2.3.23 and expanding to the first order in the ξ_j yields

$$\begin{aligned} \frac{d}{dt}C_j = (v_j'' - v_j') \left\{ (k_f \prod_{i=1}^n C_{ie}^{v_i'}) \left(1 + \sum_{i=1}^n \frac{v_i' \xi_i}{C_{ie}} \right) \right. \\ \left. - (k_b \prod_{i=1}^n C_{ie}^{v_i''}) \left(1 + \sum_{i=1}^n \frac{v_i'' \xi_i}{C_{ie}} \right) \right\} \end{aligned} \quad 2.3.25$$

But the equilibrium concentrations satisfy the condition

$$k_f \prod_{i=1}^n C_{ie}^{v_i'} = k_b \prod_{i=1}^n C_{ie}^{v_i''} = \phi \quad 2.3.26$$

so that equation 2.3.25 takes the form

$$\frac{d}{dt}C_j = -(v_j' - v_j'') \phi \sum_{i=1}^n \frac{(v_i' - v_i'') \xi_i}{C_{ie}} \quad 2.3.27$$

In order that one reaction be sufficient to characterize the composition of a mixture of n species of molecules, we must assume that these n species are formed from exactly $n - 1$ atoms. Then we can form $n - 1$ linear equations in the C_i expressing the conservation of each type of atom. These may be solved to yield

$$C_j = \alpha_j C_1 + \beta_j \quad j = 1, \dots, n \quad 2.3.28$$

where $\alpha_1 = 1$ and $\beta_1 = 0$ and we choose species 1 so that $v_1' - v_1'' \neq 0$. Then substituting 2.3.24 and 2.3.28 into 2.3.27 yields

$$\frac{d}{dt}C_j = - \frac{C_j - C_{j_e}}{\tau} \quad 2.3.29$$

where the relaxation time τ is given as

$$\frac{1}{\tau} = (v_1' - v_1'') \left(k_f \prod_{i=1}^n C_{i_e}^{v_i'} \right) \left(\sum_{i=1}^n \frac{\alpha_i}{C_{i_e}} (v_i' - v_i'') \right) \quad 2.3.30$$

If several reactions must be considered simultaneously, a similar procedure may be followed, except that one will have N_R equations of the form 2.3.27 where N_R is the number of independent reactions. From the conservation of atomic species it becomes possible to express all the concentrations in terms of at most N_R values. There results the linear system $dC/dt = B\xi$ where B is a square matrix of order N_R whose eigenvalues are the reciprocals of the relaxation times.

We note that the foregoing procedure does not provide information concerning the relative values of a_e or a_f ; it merely provides a guide to the frequency domain in which dispersion will occur due to the presence of the chemical reaction. To compute a_e and a_f it is necessary to know the complete equation of state in the form $p = p(\rho, s, C_1, \dots, C_n)$. Values of the sound speeds can be determined using the BLAKE code which accounts for real gas effects such as the covolume. Values can also be obtained using the NASA Lewis Thermochemistry Code,³⁶ but these are based on the assumption that the mixture behaves as an ideal gas.

³⁶Gordon, S. and McBride, B. J.

"Computer Program for Calculation of Complex Chemical Equilibrium Compositions, Rocket Performance, Incident and Reflected Shocks, and Chapman-Jouguet Detonations" Report No. NASA SP-273

1971

The effects of finite rate chemistry on the propagation of small disturbances have been considered by Chu³⁷ in the case of unsteady, one-dimensional flow and by Clarke³⁸ in the case of steady, supersonic, two-dimensional flow around a corner.

Of particular interest here is the solution given by Chu to the problem of the response of a quiescent column of gas, initially in chemical equilibrium, to a unit change in the value of the velocity at one boundary. This change may be thought of as due to the motion of a piston. A Laplace transform is used to determine the solution. By the method of steepest descent an approximate solution for the velocity field is found for values of $t/\tau \gg 1$ and $x/a_f\tau \gg 1$ in the form

$$\delta u = \frac{1}{2} \{ 1 + \operatorname{erf}[(t - x/a_e)/(2(a_f^2/a_e^2 - 1)\tau t)^{1/2}] \} \quad 2.3.31$$

Since the change in the boundary condition is instantaneous, high frequency components are necessarily present. Thus, a front is propagated into the gas with velocity a_f . But 2.3.31 shows that the major part of the signal propagates with velocity a_e and that δu decreases very rapidly as one proceeds from the position $x = a_e t$ towards the front of the disturbance at $x = a_f t$.

Accordingly, unless extremely sensitive detection devices are used, we expect the effective rate of signal propagation to approximate a_e rather than a_f provided that the device is located so as to satisfy $x \gg a_f \tau$. The same conclusion can be obtained from the dispersion relation 2.3.20 which shows the damping per unit length of high frequency components to be $(a_f^2 - a_e^2)/(2\tau a_f^3)$. Assuming that a_f differs significantly from a_e , the total attenuation at a distance x is $\approx \exp(-x/a_f \tau)$. If a_f is not significantly different from a_e , then, of course, the question of the relaxation time is essentially irrelevant.

A relation corresponding to 2.3.31 is deduced by Clarke³⁸ in connection with the expansion fan at a sharp corner. The streamwise component of velocity plays the role of time in a supersonic flow. Similar conclusions are deduced.

³⁷Chu, B. T.

"Wave Propagation in a Reacting Mixture"

Proc. 1958 Heat Transfer and Fluid Mechanics Institute

Univ. of California at Berkeley

1958

³⁸Clarke, J. F.

"The Linearized Flow of a Dissociating Gas"

J. Fluid Mech. 7, p. 577

1960

The present discussion has addressed systems which are always close to equilibrium. The propagation of sound in a system which is far from equilibrium has been discussed by Gilbert et al.³⁹ and by Ortoleva et al.⁴⁰

2.4 Speed of Sound in Two-Phase Flow

In the preceding section we considered the departures from ideal behavior associated with molecular structure, and, in reviewing the effects of chemical reactions, we considered the possibility that the fluid was a mixture of two or more species. In the preceding section the different constituents were assumed to be mixed at the molecular level so that a continuum representation of the behavior of the fluid retained its validity for length scales large compared with the mean free path. In the present section we consider mixtures in which heterogeneity is present at the continuum level. That is to say, there may be regions which are large compared with the intermolecular spacing and yet which contain only one or the other of the constituents. We may nevertheless treat such mixtures--suspensions of particles or droplets in a gas, or clouds of bubbles in a liquid--according to a continuum representation. However, the treatment will be strictly valid only for properties of the flow whose length scales are large by comparison with the scale of heterogeneity.

A convenient approach to the determination of governing equations for heterogeneous mixtures consisting of two distinct phases is to average the equations which govern the continuum properties of each of the constituent phases, the average being taken over a region which is large by comparison with the scale of heterogeneity. Alternatively, if the mixture is in motion so that both phases continually sweep past each fixed location, the average may be made with respect to time as is done in the theory of turbulence.⁴¹ The former approach is described

³⁹Gilbert, R. G., Hahn, H. S., Ortoleva, P. J. and Ross, J.

"The Interaction of Sound with Gas Phase Reactions"

Project Squid Tech. Rept. MIT-65-PU

1972

AD742351

⁴⁰Ortoleva, P., Gilbert, R. and Ross, J.

"Non-Equilibrium Relaxation Methods. Acoustic Effects in Transient Chemical Reactions"

Project Squid Tech. Rept. MIT-71-PU

1972

AD753798

⁴¹Hinze, J. O.

"Turbulence"

McGraw-Hill

1959

by Gough and Zwarts⁴² with particular reference to problems of interior ballistics. The latter is discussed by Ishii⁴³ and is directed towards industrial applications. The two approaches lead to identical sets of macroscopic balance equations in which the state variables are understood to represent averages of the microscopic values. The volume fractions, or fractions of a unit macroscopic volume occupied by each of the phases, are introduced as additional variables which characterize the macroscopic state of the mixture.

Although the two approaches lead to identical balance equations, questions pertaining to the resolution of such necessary constitutive laws as the representation of interphase drag and its functional dependence on the macroscopic state variables do not admit unambiguous answers.⁴⁴ The nature of sound propagation in two-phase flow is strongly regime dependent, and varying degrees of controversy attach to the choice of the constitutive laws as we pass from one regime to another.

Accordingly, we do not attempt a complete review of this topic. In view of the objective of this study, we focus our attention on a two-phase flow consisting of a compressible gas in which is suspended a dilute aggregate of small, solid particles. Thus, the results discussed here pertain specifically to the influence on the speed of sound of finely dispersed particulates arising from either incomplete combustion of the propellant or from the presence of additives whose function is other than propulsive. Care must be taken not to extrapolate these results to other types of two-phase flow such as bubbly liquids or flows in which the condensed phase has an appreciable volume loading. We will comment briefly on such cases at the conclusion of the present section.

-
- ⁴²Gough, P. S. and Zwarts, F. J.
 "Modeling Heterogeneous Two-Phase Reacting Flow"
 AIAA J. v. 17, n. 1, pp. 17-25 1979
- ⁴³Ishii, M.
 "Thermo-Fluid Dynamic Theory of Two-Phase Flow"
 Eyrolles, Paris 1975
- ⁴⁴Gough, P. S.
 "On the Closure and Character of the Balance Equations for
 Heterogeneous Two-Phase Flow"
 Dynamics and Modelling of Reactive Systems
 Academic Press 1980

The influence of an aggregate of small particles on the speed of sound in a gas has been investigated theoretically by Temkin⁴⁵ and the theoretical findings have been shown to agree very well with experimental measurements of both sound speed and attenuation.⁴⁶ The gas-phase balance equations used by Temkin⁴⁵ are as follows.

$$\frac{\partial \rho}{\partial t} + \frac{\partial \rho u}{\partial x} = 0 \quad 2.4.1$$

$$\frac{\partial u}{\partial t} + u \frac{\partial u}{\partial x} + \frac{g_o}{\rho} \frac{\partial p}{\partial x} = \frac{nF_p}{\rho} \quad 2.4.2$$

$$\frac{\partial T}{\partial t} + u \frac{\partial T}{\partial x} + \frac{p}{\rho C_v} \frac{\partial u}{\partial x} = \frac{nQ_p + nF_p(u - u_p)}{\rho C_v} \quad 2.4.3$$

These correspond with 2.1.1, 2.1.2, 2.1.3, respectively, and are clearly balances of mass, momentum and energy, in that order. We have used T, the gas-phase temperature; C_v , the gas-phase specific heat at constant volume; n the number of particles per unit volume; F_p , the velocity-dependent drag per particle; Q_p , the heat transfer per particle.

When F_p and Q_p are zero, or when n is zero, 2.4.1 and 2.4.2 are clearly identical with 2.1.1 and 2.1.2. Equation 2.4.3 is equivalent to 2.1.3, in that limit, provided that the gas is calorically perfect, as assumed by Temkin. The gas is also assumed to obey the ideal equation of state $p = \rho RT$ where R is the gas constant.

Equations 2.4.1 through 2.4.3 are applicable only in the limit when the volume fraction of the solid-phase is negligible or, alternatively, when the porosity is sufficiently close to one.

⁴⁵ Temkin, S.

"Attenuation and Dispersion of Sound by Particulate Relaxation Processes"

Division of Engineering, Brown University

Contract Nonr-562(37)

AD630326

February 1966

⁴⁶ Temkin, S. and Dobbins, R. A.

"Measurements of Attenuation and Dispersion of Sound by an Aerosol"

Division of Engineering, Brown University

Contract Nonr-562(37)

AD632911

May 1966

The particles are assumed to interact with the gas through mechanisms of drag and heat transfer, but are chemically inert. Neither combustion nor vaporization of the condensed phase is considered. The equations governing the solid-phase are

$$\frac{\partial \rho_p}{\partial t} + \frac{\partial \rho_p}{\partial x} u_p = 0 \quad 2.4.4$$

$$\frac{\partial u_p}{\partial t} + u_p \frac{\partial u_p}{\partial x} = - \frac{nF_p}{\rho_p} \quad 2.4.5$$

$$\frac{\partial T_p}{\partial t} + u_p \frac{\partial T_p}{\partial x} = - \frac{nQ_p}{\rho_p C_p'} \quad 2.4.6$$

Here we use ρ_p , the total mass of the particles per unit macroscopic volume, $\rho_p = nm_p$, where m_p is the mass of a single particle; u_p , the particle velocity; T_p , the particle temperature; and C_p' , the specific heat at constant pressure for the particles.

The equation of motion 2.4.5 is appropriate only in the limit in which the density of a specific particle is much greater than that of the surrounding gas. The buoyancy force due to the gas-phase pressure gradient is neglected. Equation 2.4.5 states that the acceleration of a particle is due solely to the velocity-dependent drag. Equation 2.4.6 is an energy balance and incorporates the assumption that the temperature within each particle is uniform at all times. This will be so only if the particles are small and have high thermal conductivity. The energy equation 2.4.6 is quite different from that used in studies of flame-spreading in granular propellant,⁴² for example, where the thermally coupled portion of the solid-phase is confined to a thin layer near the surface.

The system of equations is closed by taking the individual particles to be incompressible and by assuming the applicability of very low Reynolds number formulations of the drag and heat transfer, namely,

$$F_p = 6\pi\mu r_p (u_p - u) \quad 2.4.7$$

$$Q_p = 4\pi k_c r_p (T_p - T) \quad 2.4.8$$

where r_p is the particle radius; μ is the viscosity of the gas-phase; and k_c is the thermal conductivity of the gas-phase.

Corresponding to these forms for the interphase couplings due to

drag and heat transfer are the natural time scales for the respective relaxation phenomena, namely

$$\tau_d = m_p / 6\pi\mu r_p \quad 2.4.9$$

which is the characteristic relaxation time for velocity differences and

$$\tau_t = C'_p m_p / 4\pi r_p k_c \quad 2.4.10$$

which is the characteristic relaxation time for temperature differences. It may be noted that $\tau_t = (3/2)(C'_p/C_p)Pr\tau_d$ where Pr , the Prandtl number is approximately equal to one for gases. In general, therefore, τ_t and τ_d are of the same order of magnitude.

The roles played by τ_d and τ_t become especially clear when we now consider a perturbation of the balance equation about a uniform, quiescent state, denoted by subscript o . The small perturbations are denoted by subscript 1 . Then 2.4.5 and 2.4.6 become

$$\frac{\partial u_{p1}}{\partial t} = -(u_{p1} - u_1)/\tau_d \quad 2.4.11$$

$$\frac{\partial T_{p1}}{\partial t} = -(T_{p1} - T_1)/\tau_t \quad 2.4.12$$

The similarity to equation 2.3.13 should be noted.

When 2.4.1-2.4.8 are linearized and a Fourier dependence $\exp i(kx - \omega t)$ is assumed for each of the state variables, the condition of solvability for the resulting linear homogeneous system determines k as a function of ω . In the limit when $C_m^2 = (n_o m_p / \rho_o)^2 \ll 1$, or, in other words, for very low mass concentrations of the solid-phase, it is found that⁴⁶

$$\text{Re}\left(\frac{\omega}{k}\right) = a_o \left\{ 1 + C_m \left[\frac{1}{1 + \omega^2 \tau_d^2} + \frac{(\gamma - 1)(C'_p/C_p)}{1 + \omega^2 \tau_t^2} \right] \right\}^{-1/2} \quad 2.4.13$$

where $a_o = (\gamma g_o p_o / \rho_o)^{1/2}$ is the speed of sound in the gas, and

$$\text{Im}\left(\frac{\omega}{k}\right) = \frac{C_m \omega}{2a_o} \left\{ \frac{\omega \tau_d}{1 + \omega^2 \tau_d^2} + (\gamma - 1)(C'_p/C_p) \frac{\omega \tau_t}{1 + \omega^2 \tau_t^2} \right\} \quad 2.4.14$$

and it will be recalled that $\text{Re}(\omega/k)$ is the phase velocity while $\text{Im}(\omega/k)$ is the attenuation per unit length.

From 2.4.13 it follows that the equilibrium and frozen sound speeds may be determined as

$$a_e = \lim_{\omega \rightarrow 0} \text{Re}\left(\frac{\omega}{k}\right) = a_o [1 + C_m (1 + (\gamma - 1)(C'_p/C_p))]^{-1/2} \quad 2.4.15$$

and

$$a_f = \lim_{\omega \rightarrow \infty} \text{Re}\left(\frac{\omega}{k}\right) = a_o \quad 2.4.16$$

Thus, the presence of a very dilute suspension exerts no influence on the rate of propagation of high frequency components. But the damping per unit length satisfies

$$\lim_{\omega \rightarrow \infty} \text{Im}\left(\frac{\omega}{k}\right) = \frac{C_m}{2a_o \tau_d} [1 + (\gamma - 1)(C'_p/C_p)] \frac{\tau_d}{\tau_t} \quad 2.4.17$$

while the limit as $\omega \rightarrow 0$ is evidently zero. Thus, we may expect that a signal consisting of a sudden jump in a boundary value will propagate similarly to that in a reacting mixture as described in the preceding section. The signal front will propagate at a_f but with ever increasing attenuation due to dissipation, so that the bulk of the signal will propagate at the velocity a_e . As with the case of the chemically reacting flow, the definition of signal speed is unambiguous only if the instrumentation used to detect the signal is allowed to have arbitrarily high sensitivity.

It should be noted that 2.4.17 agrees with the general result 2.3.20 when either mechanical or thermal relaxation is considered as a sole nonequilibrium process.

We should also mention that the mathematical limit $\omega \rightarrow \infty$ is, of course, subject to constraints arising from the validity of the equations. We have already mentioned that the continuum viewpoint is appropriate only for sufficiently large scale and slow processes. Temkin⁴⁵ also points out that the constitutive relations 2.4.7 and 2.4.8 require for their validity $\omega \tau_d \lesssim 1$ and $\omega \tau_t \lesssim 1$, respectively, in addition to the Reynolds number limit $\text{Re}_p = \rho |u - u_p| r_p / \mu \lesssim 1$.

The frozen and equilibrium sound speeds for a two-phase flow in which the compressibility and concentration of each species are significant

are given by Wallis,⁴⁷ in connection with a discussion centered on stratified flow. It is easy to show that these relations are also valid for mixtures consisting of interpenetrating phases such as bubbly flow or a flow involving a dense, but dispersed, aggregate of particles, provided that the phases are only coupled mechanically. Using subscripts 1 and 2 to distinguish the two phases, α to denote the volume fraction, ρ the density and a the speed of sound in each medium alone, we have⁴⁷

$$a_f^2 = \frac{\alpha_1/\rho_1 + \alpha_2/\rho_2}{\alpha_1/\rho_1 a_1^2 + \alpha_2/\rho_2 a_2^2} \quad 2.4.18$$

and

$$1/a_e^2 = (\alpha_2 \rho_2 + \alpha_1 \rho_1) \left(\frac{\alpha_1}{\rho_1 a_1^2} + \frac{\alpha_2}{\rho_2 a_2^2} \right) \quad 2.4.19$$

It should be noted that a_f lies between a_1 and a_2 . However, the same is not necessarily true of a_e which may, in certain cases, be significantly smaller than either a_1 or a_2 . For example, Eddington reports a velocity of 66 fps for a homogeneous mixture of water and air.⁴⁸ In such a mixture, undergoing acoustic vibrations slow enough to maintain mechanical equilibrium between the phases, the propagation rate tends to be controlled by the inertia of the condensed phase and the bulk modulus of the gas-phase.

The reason for the validity of 2.4.18, 2.4.19 in the context of two-phase systems other than stratified flow is due to the fact that neither the frozen nor the equilibrium sound speed depends on the details of the interphase couplings, provided that they are algebraic in nature. If the interphase drag depends on the rate of change of the flow, however, the frozen value may be affected although the equilibrium value will not. The influence of a differential constitutive term on the frozen sound speed is easy to understand from the identification of the frozen value with the characteristic value as discussed in section 2.2.

⁴⁷Wallis, G. B.

"One-Dimensional Two-Phase Flow"

McGraw-Hill

1969

⁴⁸Eddington, R. B.

"Investigation of Supersonic Phenomena in a Two-Phase (Liquid-Gas)

Tunnel"

AIAA J. vol. 8, n. 1, pp. 65-74

January 1970

Further details of the influence of such a differential effect, the virtual mass contribution to drag, may be found in the work of Gough.⁴⁹

We also note that 2.4.18, 2.4.19 agree with 2.4.16 and 2.4.15, respectively when $\alpha_1 \approx 1$, $\alpha_2 \ll 1$, $\rho_1 \ll \rho_2$, $a_2 \rightarrow \infty$ and when the thermal coupling term involving C'_p/C_p in 2.4.15 is neglected.

⁴⁹Gough, P. S.

"The Flow of a Compressible Gas Through an Aggregate of Mobile, Reacting Particles"
PhD Thesis, McGill University

1974

3.0 PROPAGATION OF THE MUZZLE RAREFACTION WAVE

We turn now to a discussion of the behavior of the rarefaction induced by the discharge of the projectile from the gun. Of course, a necessary condition that such a wave travel backwards towards the breech is that the velocity of the projectile be less than the speed of sound in the gas directly behind it at the instant of discharge. If such is the case, then the gas in the vicinity of the muzzle is strongly accelerated by the differential between the in-bore pressure and the relatively low external pressure. As we discussed in chapter 1.0, due to the precursor shock, the external pressure may be higher than atmospheric but it will still be significantly less than the base pressure.

Concurrently with the acceleration of the gas in the vicinity of the muzzle, the expansion wave moves rearward through the barrel. The rearward propagating wave is detected by means of pressure gages mounted on the sidewall of the barrel. From the known spacing between the gages and the time correlation of the pressure gage data, the wave velocity is determined. The speed of sound follows by eliminating the contribution of the motion of the gas to the net measured wave velocity. Then the equation of state of the gas is used to determine the temperature from the speed of sound.

Let us now consider the factors influencing the wave motion in somewhat greater detail. We first discuss qualitative details of the wave structure and subsequently consider quantitative details insofar as we are able at present. The quantitative discussion is centered on a specific ballistic configuration, namely, a 155 mm zone 5 propelling charge.

The qualitative behavior of the muzzle rarefaction is sketched in Figure 3.1. We depict the situation at the instant of muzzle exit, shortly thereafter when the expansion has just reached the centerline, and still later when the expansion wave has traveled rearward a distance of 1 or 2 calibers.

At the instant prior to the exit, the flow consists of an essentially one-dimensional core contained within a thin developing boundary layer at the wall and terminated near the projectile base by a weak radially outward flow, the precise structure of which appears to depend on such geometric details as the magnitude of the gap between the projectile and the tube.⁵⁰ Due to the relatively short time associated with

⁵⁰Stuhmiller, J. H. and Ferguson, R. E.

"Calculations of Internal Ballistic Flow with a Projectile to Wall Gap"

Ballistic Research Laboratory Contract Report ARBRL-CR-00463 August 1981
(ADA 104632)

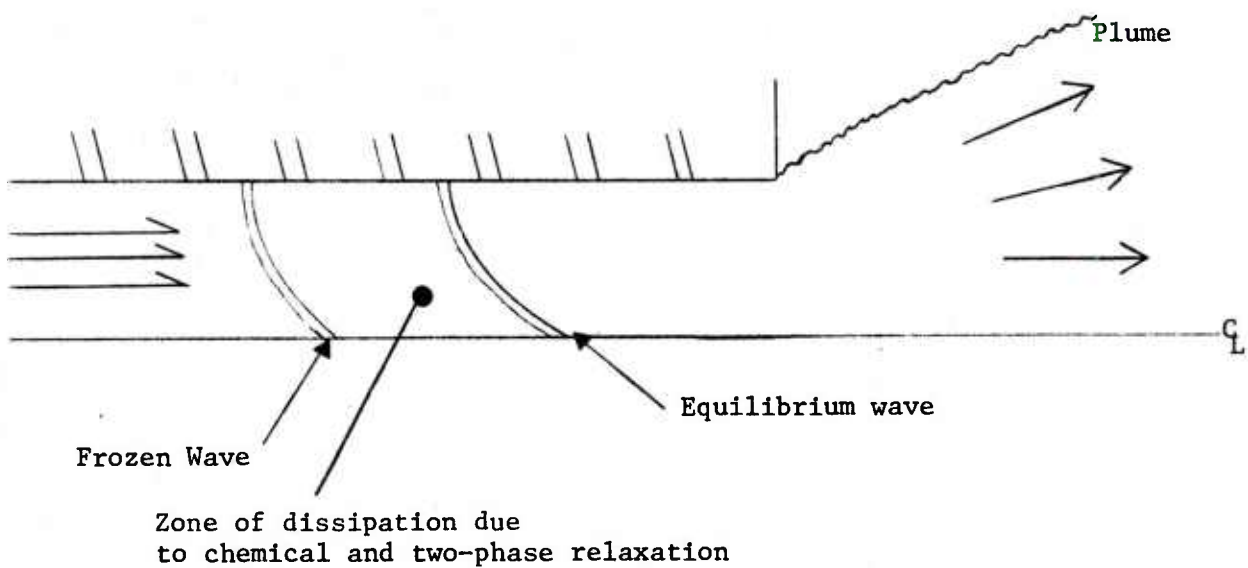
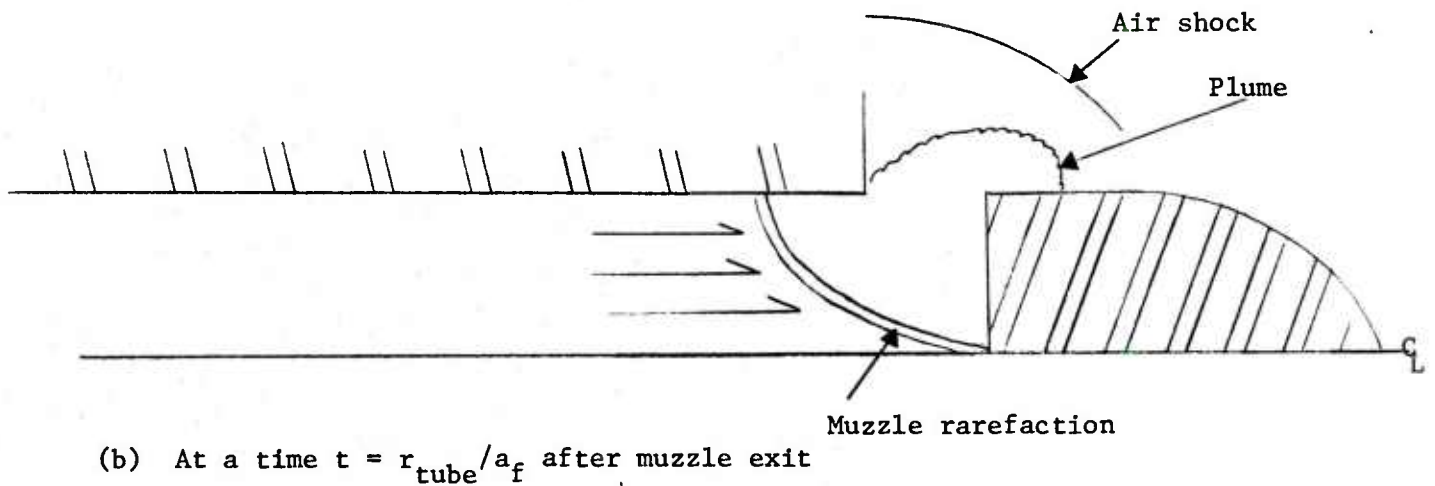
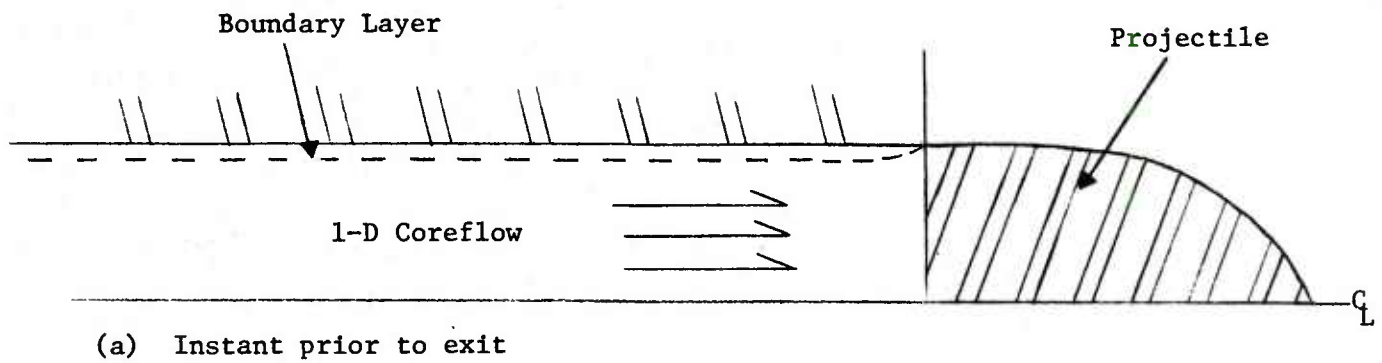


Figure 3.1 Qualitative Behavior of Muzzle Rarefaction Wave

the internal ballistic event, the boundary layer at the wall is expected to be very thin. Calculations by Shelton et al⁵¹ show the momentum thickness of the developing boundary layer in a 30 mm cannon to be less than 3% of the tube radius. Their calculations were based on data which implicitly assumed a fully developed turbulent structure. It has been suggested by Stuhmiller⁵¹ that the time frame involved is, in fact, too short to allow fully developed turbulent structure. This would imply that the effective diffusivity will therefore be less than is assumed in the model of Shelton et al and that the actual boundary layer thickness may therefore be less than their estimate. The fraction of the tube occupied by the boundary layer is also expected to vary inversely with the tube diameter.

Accordingly, to a degree of accuracy which exceeds that of other aspects of this problem, we may view the flow at the instant prior to muzzle exit as one-dimensional with uniform radial properties.

When the projectile clears the barrel a strong annular expansion is propagated into the tube while the emerging gas expands outwards and around the projectile, initiating the air shock or blast wave as discussed in chapter 1.0. During the period immediately after the discharge of the projectile, the muzzle rarefaction has considerable two-dimensional structure. It travels rearwards at an absolute velocity equal to $u - a$, where u is the gas velocity, and inward with the velocity $-a$. Since the change in pressure at the lip of the tube is, in principle, instantaneous, the rarefaction is a characteristic wave and the leading edge travels at the frozen speed of sound. We have therefore used the symbol a_f in Figure 3.1 (b) to denote the wave front.

As the wave travels rearward, the front tends to become planar and the relaxation wave becomes one-dimensional. Behind the leading edge, which travels with the frozen speed of sound, is a region of dissipation in which the internal modes of the gas adjust to the suddenly imposed change of state and also, possibly, in which two-phase dissipative processes are at work. Some distance behind the frozen wave front is the equilibrium wave which will tend to convey the signal with much greater strength than the frozen wave, particularly as the time of passage becomes large compared with the relaxation times of the various internal and two-phase departures from local equilibrium.

Ideally, with perfect mechanical tolerances, the discharge would be a truly instantaneous event. The frozen wave speed would therefore involve freezing of the rotational and vibrational degrees of freedom of the individual molecules as well as of the overall composition. We may already anticipate from the discussion of chapter 2.0 that the relaxation time of the rotational modes is so short that very little of

⁵¹Shelton, S., Bergles, A., and Saha, P.
"Study of Heat Transfer and Erosion in Gun Barrels"
AFATL-TR-73-69

March 1973

the signal energy is likely to be present in the completely frozen front as it passes successive gage locations. In order to confirm this point and to assess the roles of the other nonequilibrium processes, we now consider a specific numerical example.

The following table specifies the composition of the gas at the muzzle as computed using the BLAKE code for a 155 mm zone 5 propelling charge.

Composition of Gas at Muzzle of 155 mm Gun⁵²

CO	20.44 gm-mol/kgm
H ₂	9.44
H ₂ O	4.55
N ₂	4.40
CO ₂	4.18
CH ₄	0.61
KOH	0.12
Others	< 0.09

The mixture is characterized by the following values.

Pressure:	p = 19.0 MPa
Density:	$\rho = 0.0346 \text{ gm/cm}^3$
Temperature:	T = 1450°K
Ratio of Specific Heats	$\gamma = 1.279$
Molecular Weight:	$M_w = 22.818 \text{ gm/gmol}$
Covolume:	b = 1.17

⁵²Keller, G.
Private Communication

From these data we may determine the isentropic sound speed-- with rotational and vibrational equilibrium, but with frozen composition-- according to the formula

$$a = \left\{ \frac{\gamma g_o p / \rho}{1 - b p} \right\}^{1/2} \quad 3.1$$

which yields $a = 857$ m/sec. The viscosity may be estimated from the Sutherland formula

$$\mu = 0.1340(T/298)^{1.5} / (T + 110) \quad 3.2$$

which yields $\mu = 9. \times 10^{-4}$ gm/cm-sec. From equation 2.3.8 we may estimate the mean free path as $\lambda \sim 9.33 \times 10^{-7}$ cm, and taking the average translational velocity to be equal to the speed of sound yields the mean free time $\tau_{trans} \sim 10^{-11}$ sec. Therefore, relaxation of the distribution of translational velocities to a Maxwell distribution occurs in a characteristic time of the order of 10^{-11} sec. From the discussion of section 2.3.2.2 we see that rotational relaxation of H_2 requires approximately 300 collisions so that $\tau_{rot} \sim 3 \times 10^{-9}$ sec for the muzzle exit conditions. The vibrational relaxation time of carbon monoxide, a significant constituent in the present example, may be estimated as $\tau_{vib} \sim 3 \times 10^{-6}$ sec. This value follows from the cited value of $\tau_{vib} \sim 5.5 \times 10^{-4}$ sec at 1 atmosphere and the inverse dependence on pressure, the present example involving a pressure of 188 atmospheres. This value $\tau_{vib} \sim 3 \times 10^{-6}$ sec is likely to represent an upper bound for all the constituents since carbon monoxide is known to relax slowly, and, moreover, we have not considered the reduction in τ_{vib} which follows from the presence of other molecules, as discussed in section 2.3.2.2.

The estimation of the chemical relaxation time is complicated by the large number of possible reactions which may occur and also by the state of knowledge of the reaction rates. To estimate the approximate magnitude of the chemical relaxation time and also the degree of uncertainty which attaches to the estimate, we consider one overall reaction, the so-called water-gas reaction



and we consider two alternative paths to the computation of the relaxation time for this reaction.

We consider first an overall Arrhenius form for the reaction which has been tabulated by Westley⁵³ as

$$k_f = AT^B \exp (-E/RT) \quad 3.4$$

with $A = 10^9$, $B = 0.5$, $E/R = 7550$ in gmol, cm, sec, °K units, valid from 1500-2500°K with range of uncertainty $0.3k_f < k < 3.2k_f$ where k is the actual value and k_f is as given by 3.4.

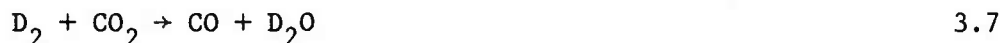
We use Equation 2.3.30, evaluating the stoichiometric coefficients v_i' and v_i'' from 3.3 and the α_i from separate balances of C, O and H. Then, using [] to denote molar concentration we have

$$\frac{1}{\tau_{wg}} = k_f [\text{CO}_2] [\text{H}_2] \left\{ \frac{1}{[\text{CO}_2]} + \frac{1}{[\text{H}_2]} + \frac{1}{[\text{CO}]} + \frac{1}{[\text{H}_2\text{O}]} \right\} \quad 3.5$$

Using the BLAKE code results for the molar quantities per kgm and the mixture density of 0.0346 gm/cm³ determines the molar concentrations. Equation 3.4 yields the value of k_f at 1450°K and then Equation 3.5 yields

$$\tau_{wg} = 5.7 \text{ } \mu\text{sec} \quad 3.6$$

An alternative estimate of the relaxation time may be made using data supplied by Brupbacher et al⁵⁴ who measured the approach to equilibrium of the reaction*



⁵³Westley, F.

"Table of Recommended Rate Constants for Chemical Reactions Occurring in Combustion"

NSRDS-NBS67

April 1980

⁵⁴Brupbacher, J. M., Kern, R. D. and O'Grady, B. V.

"Reaction of Hydrogen and Carbon Dioxide Behind Reflected Shock Waves"

J. Phys. Chem. vol. 80, n. 10, pp. 1031-1035

May 1976

*The author is indebted to Dr. J. Heimerl of BRL who drew his attention to reference 54 and who provided several useful criticisms of the work discussed in this section.

It was found that

$$X_{D_2O}/X_{D_2O,eq} = 1 - \exp \{-k [D_2]^{0.3} [M]^{0.7} t^2\} \quad 3.8$$

for $2275^\circ K \leq T \leq 3860^\circ K$ with X = mole fraction, M = Argon and $k = 10^{20} \exp (-81.4/RT) \text{ cm}^3\text{-mole}^{-1}\text{-s}^{-2}$. The form of Equation 3.8, which was selected to fit the observed overall relaxation process, is somewhat different from that which would be expected from the Mandelshtam-Leontovich formulism. Equation 3.7 evidently involves a characteristic time

$$\frac{1}{\tau} = (k[D_2]^{0.3} [M]^{0.7})^{1/2} \quad 3.9$$

If it is assumed that 3.9 is valid for H_2 rather than D_2 , for $[M] = [CO_2] + [CO] + [N_2] + [H_2] + [H_2O]$ rather than Argon, and for $T = 1450^\circ K$, it follows that the water-gas reaction has the relaxation time

$$\tau_{wg} = 0.44 \text{ msec} \quad 3.10$$

The estimates of the relaxation time associated with just one possible chemical reaction both yield values larger than those pertinent to the internal molecular modes considered previously, and the second estimate 3.10 is much larger. Corresponding to each relaxation time, we may estimate a relaxation length $\delta \sim a\tau$, and we summarize the foregoing in the following table.

Process	Relaxation Time sec	Relaxation Length cm
Establish Maxwell Distribution	10^{-11}	8.6×10^{-7}
Equilibrate Rotational Modes	3×10^{-9}	2.6×10^{-4}
Equilibrate Vibrational Modes	3×10^{-6}	0.26
Equilibrate Water-Gas Reaction	5.7×10^{-6}	0.49 (Ref. 53)
	4.4×10^{-4}	38.1 (Ref. 54)

Now although we are unable to provide a quantitative estimate of the spectral content of the unloading wave, we may observe from an inspection of typical pressure records⁵⁵ that the data resolution limit is $\geq 2 \times 10^{-5}$ sec. Hence, the relaxation layers for the vibrational, rotational and translational modes will be too thin to be resolved by the instrumentation. Only the relaxation time for the water-gas reaction as estimated from the data of reference 54 is large enough to be resolved experimentally.

From the two estimates of τ_{wg} we may draw a number of conclusions. If the estimate based on reference 53 is correct, we could assume the water-gas reaction to be in equilibrium. For, the muzzle velocity is 386 m/sec in the present example, so that the wave speed relative to the gages is approximately 469 m/sec. The distance between the first and the last of the gages is 15 cm so that the wave transit time is 0.32 msec, which is much larger than τ_{wg} according to the first estimate. But, according to the second estimate of τ_{wg} based on reference 54, we have τ_{wg} almost exactly equal to the event time τ_{meas} . Hence, if the second estimate is correct, we can expect that the water-gas reaction, at least, would introduce dispersion of the unloading wave, and the effective wave speed would therefore lie between the frozen and equilibrium values. Since we do not know which of the two estimates is closer to the truth, we conclude that wave dispersion due to the finite chemical rates of reaction represents a source of experimental error which can neither be ruled out nor compensated without further study. Moreover, we note that Brupbacher et al attempted to model the overall reaction 3.7 using a total of eleven elementary reactions. Although the theoretical time dependence was found to accord with 3.8 in a functional sense, the theoretical and experimental rate constants were found to differ markedly. Hence, we conclude that if further study is directed towards the elucidation of the degree of wave dispersion induced by finite rate chemistry, the analysis will be complex and not necessarily fruitful.

Pending such further study, it is concluded that the data reduction scheme must accept as a source of uncertainty the difference between the equilibrium and frozen sound speeds of the mixture. In general, the inversion of the equation of state to deduce the temperature from the speed of sound must be performed twice, first assuming the composition to be frozen, and second, assuming it to be in equilibrium. In the present example it appears that the resulting uncertainty in temperature is 4% or approximately 60°K.

⁵⁵Keller, G. E. and Schmidt, E. M.

"Gun Muzzle Gas Temperature Measurements Using Acoustic Thermometry--A Progress Report"
Proceedings of the 17th JANNAF Combustion Meeting

1980

So far we have discussed molecular contributions to the dispersion of the unloading wave. But geometrical dispersion will also be present. We observe that the characteristic time for the rarefaction to spread through the exit plane cross section is $\tau_r = 0.18$ msec. The significance of τ_r is as follows. The components with frequency $\omega \gg \tau_r^{-1}$ will be strongly attenuated as the unloading wave moves rearward. Such high frequency components will be associated with the initial unloading of the propellant gas at the lip of the tube and will propagate as diverging waves with amplitude decaying in proportion to the distance from the source. Thus, while the high frequency components will not necessarily be strongly damped by the chemical reaction 3.3, they will be damped by geometrical factors. Assuming a fixed level of sensitivity of the instrumentation, it follows that the faster chemically frozen wave will be less susceptible to detection as it propagates rearward subject to strong geometrical dispersion. Accordingly, the apparent speed of sound will decrease from a frozen value near the muzzle to the equilibrium value as it passes successive gages. Unfortunately, we are not in a position to quantify this discussion.

Even when the wave has become essentially one-dimensional, we note that its effect on successive pressure gages decreases with rearward motion. Initially, the pressure drops sharply since the velocity must increase suddenly from $\sim 0.5 a_f$ to $\sim a_f$. But as the wave spreads, the adjustment that it imposes on the flow progressively weakens, and the inflection of the pressure history at successive gages becomes increasingly difficult to observe. This effect may result in an apparent speed of sound which is less than the equilibrium value.

While the apparent sound speed is expected to decrease with rearward propagation due to chemical and geometrical dispersion, the influence of the velocity distribution may compensate sufficiently as to produce an apparent increase in the absolute speed of the signal relative to the gun tube. The velocity of the gas decreases as we move rearward so that the absolute wave speed $u - a$ tends to larger negative values.

The influence of the gas velocity may be eliminated from the observed absolute wave speed by means of the following argument which is offered as an alternative to the method used by Schmidt.¹ To a high degree of approximation, the gas velocity distribution varies linearly between the value 0 at the breech and the value $\dot{x}_p(t)$ at the base of the projectile $x_p(t)$. Thus

$$u(x, t) = x_p \frac{\dot{x}_p(t)}{x_p(t)} \quad 3.11$$

This relation which applies throughout the barrel prior to the discharge of the projectile* will continue to apply, following muzzle exit, to that portion of the gas which has not yet been influenced by the unloading wave. We have merely to continue the values of x_p and \dot{x}_p in time as though the projectile were still subject to propulsion. Using a subscript m to denote muzzle conditions, we can write the following approximate relations for x_p and \dot{x}_p when $t \geq t_m$, the muzzle exit time

$$\dot{x}_p = \dot{x}_{pm} + (A_p g_o / M_p)(t - t_m) \quad 3.12$$

$$x_p = x_m + \dot{x}_{pm}(t - t_m) + \frac{1}{2}(A_p g_o / M_p)(t - t_m)^2 \quad 3.13$$

where A is the tube area and M_p is the mass of the projectile.

An additional point to consider in respect to this form of acoustic thermometry is that the temperature measurement is confined to a sample of gas within one or two calibers from the base of the projectile at the instant of muzzle exit. Yet the temperature in this location may differ appreciably from the values obtained throughout the bulk of the tube. Since the air blast is dependent not only on the initial energy flux, but on the entire history of the energy flux, the acoustic thermometric value may not be appropriate as a means of characterizing the likelihood of the charge to exceed a certain threshold of blast intensity or to induce secondary combustion in the atmosphere. Unfortunately, the deviation of the temperature near the projectile base from the space-mean value throughout the tube may be either to higher or to lower values, and, in fact, is dependent on the detailed distribution of the solid propellant during the combustion cycle.

In the present instance, a numerical solution of the two-phase reacting mixture equations by means of the NOVA code⁵⁶ indicates that the temperature takes the value 1705°K for a distance of 2-3 calibers behind the projectile. The remainder of the gas is generally a good deal cooler, being approximately at 1440-1550°K. A similar phenomenon has been predicted by Heiser and observed experimentally by Klingenberg.⁵⁷

⁵⁶ Gough, P. S.

"The NOVA Code: A User's Manual"
IHCR-80-8

December 1980

⁵⁷ Klingenberg, G. and Mach, H.

"Experimental Study of Non-Steady Phenomena Associated with
the Combustion of Solid Gun Propellants"
16th Symposium on Combustion, MIT

August 1976

*The distribution 3.11 may fail to be realized very early in the ballistic cycle when the propellant is being ignited. But it will apply as the projectile approaches the muzzle, even if the propellant is not entirely consumed.

The spatial variation of temperature is a result of nonuniform heat addition, and it is easy to see that, depending on the detailed history of heat addition near the base of the projectile, the temperature at muzzle exit can be either elevated or depressed relative to the bulk value.

Thus far, we have said nothing concerning the influence of a dispersed particulate phase. In the present example the propellant is found to be completely consumed. For the sake of completeness, however, we will briefly consider the magnitude of the relaxation time τ_d due to the drag exerted by very small particles. We will be assuming that the interphase drag is therefore in the viscous-dominated regime, and these results will not be applicable to flows involving large propellant grains which are but fractionally burnt. In the same regime of small, dispersed particles we will also examine the values of the frozen and equilibrium sound speeds as a function of particle concentration.

From Equation 2.4.9 with the arbitrary assumption that the particle density is 1 gm/cm^3 we see that $\tau_d = (2/9)(r_p^2/\mu)$, and as computed previously, the value of $\mu \sim 9 \times 10^{-4}$.

Thus, we have the following table of values of τ_d as a function of r_p , the particle radius.

r_p (cm)	τ_d (sec)
10^{-4}	2.47×10^{-6}
10^{-3}	2.47×10^{-4}
10^{-2}	2.47×10^{-2}
10^{-1}	2.47
1	2.47×10^2

Accordingly, only particles smaller than 10^{-3} cm can be expected to remain in mechanical equilibrium for an unloading wave of the type considered in the present chapter. The millimeter and centimeter sized particles are included in the table only for interest's sake. Particles of those sizes would almost certainly require consideration of high Reynolds number drag.

We turn now to the influence of particle concentration on the frozen and equilibrium speeds of sound. Using subscript 1 to refer to the gas and subscript 2 to refer to the particles, we will assume $\alpha_1 \approx 1$, $\alpha_2 \ll 1$, $\rho_2 \gg \rho_1$ and $a_2 \gtrsim a_1$. Then Equations 2.4.18 and 2.4.19 take the approximate forms:

$$a_f/a_1 \approx (1 + \frac{\alpha_2 \rho_1}{\rho_2} (1 - \frac{a_1^2}{a_2^2}))^{1/2} \quad 3.14$$

$$a_e/a_1 \approx (1 + \frac{\alpha_2 \rho_2}{\rho_1})^{-1/2} \quad 3.15$$

Evidently, when $a_1 = a_2$ we have $a_f/a_1 = 1$, so that a conservative estimate of a_f may be made with $a_2 \rightarrow \infty$ whereupon

$$a_f/a_1 \approx (1 + \frac{\alpha_2 \rho_1}{\rho_2})^{1/2} \quad 3.16$$

In the present example $\rho_1 = 0.0346 \text{ gm/cm}^3$ and, to be consistent with the calculations of τ_d , we will suppose $\rho_2 = 1 \text{ gm/cm}^3$. Then we may construct the following table of values of a_f/a_1 , a_e/a_1 as a function of the concentration by volume α_2 of the particles.

α_2	a_f/a_1	a_e/a_1
10^{-3}	1.0000	0.986
10^{-2}	1.0002	0.881
10^{-1}	1.0017	0.507

Evidently, the frozen wave speed is hardly affected at all by the presence of particles with volume concentration as large as 0.1. On the other hand, the equilibrium wave speed may be sharply reduced. Of course, a concentration of 0.1 is likely to be associated with centimeter sized particles for which the relaxation time may be so large that the equilibrium condition is not relevant to the measurement. If discharges involving high volume concentrations of solids are of interest, the NOVA code may be used to simulate the unloading event. The full nonlinear solution may be determined, including the effects of Reynolds number dependent drag, virtual mass effect and gas-phase discharge conditions.

4.0 CONCLUSIONS

In the present study we have considered certain sources of error which attach to the determination of the temperature of the propellant gas at muzzle exit from measurements of the speed of the unloading wave. The accuracy with which the equation of state itself is known has not been addressed. The sources of error considered here have been associated with the finite rates of equilibration of the internal modes of the gas, the presence of dispersed particulates, and the lack of uniformity of the properties of the flow.

For a particular example, involving no particulates, it has been concluded:

- (1) The translational, rotational and vibrational modes of the gas are in equilibrium as far as the unloading wave is concerned.
- (2) It is uncertain whether the composition of the gas is frozen or in equilibrium during the unloading event. Inversion of the equation of state to deduce the temperature of the gas from the speed of sound yields values which differ by 4% or approximately 60°K when the chemistry is first assumed to be frozen and subsequently to be in equilibrium.
- (3) A computer simulation based on a two-phase interior ballistic model shows that the temperature is anomalously high near the projectile base. A temperature of ~1705°K is predicted for a region extending 2-3 calibers behind the projectile while the balance of the gas is cooler, being at 1440-1550°K. Hence, a determination of the temperature near the muzzle will yield an anomalously high value relative to that in the bulk of the gas in the particular example considered here.
- (4) The geometrical dispersion due to the two-dimensional geometry of the unloading wave is too complicated to quantify as a source of error without further study.

With regard to the general application of the technique considered here, we conclude as follows:

- (1) Pending further analysis, which would certainly be complex, it appears that the equation of state must be inverted, in general, first on the assumption that the chemistry is frozen and second that it is in equilibrium. The resulting difference in temperature must be accepted as an experimental uncertainty.
- (2) Because the propagation of the unloading wave is studied in a region of gas adjacent to the projectile base, there is a strong possibility that the temperature deduced from such data will differ significantly from that in the bulk of the propellant gas. The deviation may be to higher or lower values and depends on the detailed history of the distributed heat release of the propellant. Caution should therefore be exercised in respect to:

- (a) The use of the measured temperature to predict the probability and intensity of secondary combustion.
- (b) Comparisons between the measured temperature and predictions made using lumped parameter interior ballistic codes.

References

1. Schmidt, E. M., Gion, E. J., and Shear, D. D.
"Acoustic Thermometric Measurements of Propellant Gas
Temperatures in Guns"
AIAA J., vol. 15, no. 2, pp. 222-226 February 1977
2. Schmidt, E. M., Gion, E. J. and Fansler, K. S.
"Analysis of Weapon Parameters Controlling the
Muzzle Blast Overpressure Field"
Fifth International Symposium on Ballistics April 1980
3. Oswatitsch, K.
"Intermediate Ballistics"
DVL Report 358, June 1964,
Deutschen Versuchsanstalt fur Luft und Raumfahrt
Aachen, Germany
AD 473-249
4. Schmidt, E. M. and Shear, D. D.
"Optical Measurements of Muzzle Blast"
AIAA J., vol. 13, no. 8, pp. 1086-1091 August 1975
5. Erdos, J. I. and Del Guidice, P. D.
"Calculations of Muzzle Blast Flowfields"
AIAA J., vol. 13, no. 8, pp. 1048-1055 August 1975
6. Klingenberg, G.
"Investigation of Combustion Phenomena Associated
with the Flow of Hot Propellant Gases. III:
Experimental Survey of the Formation and Decay of
Muzzle Flow Fields and of Pressure Measurements"
Combustion and Flame, vol. 29, no. 3 1977
7. Celmins, A.
"Theoretical Basis of the Recoilless Rifle Interior
Ballistic Code, RECRIF"
Ballistic Research Laboratory Report 1931 September 1976
(ADB 013832L)
8. Liepmann, H. W. and Roshko, A.
"Elements of Gasdynamics"
John Wiley and Sons 1957

9. Klingenberg, G. and Mach, H.
 "Investigation of Combustion Phenomena Associated
 with the Flow of Hot Propellant Gases - I: Spectro-
 scopic Temperature Measurements Inside the Muzzle
 Flash of a Rifle"
 Combustion and Flame, vol. 27, no. 2 October 1976

10. Klingenberg, G. and Schröder, G. A.
 "Investigation of Combustion Phenomena Associated
 with the Flow of Hot Propellant Gases - II: Gas
 Velocity Measurements by Laser-Induced Gas Breakdown"
 Combustion and Flame, vol. 27, no. 2 October 1976

11. Yagla, Jon J.
 "Analysis of Gun Blast Phenomena for Naval Architecture,
 Equipment, and Propellant Charge Design"
 Third International Symposium on Ballistics,
 Karlsruhe, Germany March 1977

12. Carfagno, S. P.
 "Handbook on Gun Flash"
 The Franklin Institute November 1961

13. Heiney, O. K. and Powers, R. J.
 "Secondary Muzzle Gas Combustion Considerations
 in Aircraft Cannon"
 Proceedings of the 14th JANNAF Combustion Meeting August 1977

14. May, I. W. and Einstein, S. I.
 "Prediction of Gun Muzzle Flash"
 Proceedings of the 14th JANNAF Combustion Meeting August 1977

15. Yousefian, V. and May, I. W.
 "Prediction of Muzzle Flash Onset"
 Proceedings of the 16th JANNAF Combustion Meeting 1979

16. Smith, F.
 "A Theoretical Model of the Blast From Stationary
 and Moving Guns"
 First International Symposium on Ballistics
 Orlando, Florida November 1974

17. Westine, P.
 "The Blast Field About the Muzzle of Guns"
 Shock and Vibration Bulletin, vol. 39, part 6 March 1969

18. Schmidt, E.
 "Survey of Muzzle Blast Research"
 Fifth International Symposium on Ballistics April 1980

19. Strutt, J. W. (Baron Rayleigh)
"The Theory of Sound" vol. II.
Dover Publications 1945
20. Goldstein, H.
"Classical Mechanics"
Addison-Wesley 1959
21. Blackstock, D. T.
"History of Nonlinear Acoustics and a Survey of
Burgers' and Related Equations"
in Nonlinear Acoustics, Proceedings of a Conference at
Applied Research Laboratories, University of Texas at
Austin
AD 719936 1969
22. Shapiro, A. H.
"The Dynamics and Thermodynamics of Compressible
Fluid Flow"
Ronald Press 1953
23. Courant, R. and Friedrichs, K. O.
"Supersonic Flow and Shock Waves"
Interscience 1948
24. Petrovsky, I. G.
"Partial Differential Equations"
Interscience 1954
25. Landau, L. D. and Lifshitz, E. M.
"Fluid Mechanics"
Pergamon Press 1959
26. Fung, Y. C.
"Foundations of Solid Mechanics"
Prentice-Hall 1965
27. Jackson, J. D.
"Classical Electrodynamics"
John Wiley and Sons 1962
28. Gough, P. S.
"Fundamental Investigation of the Interior Ballistics
of Guns"
Naval Ordnance Station, Indian Head, MD
IHCR 74-1 1974

29. Ramshaw, J. D. and Trapp, J. A.
 "Characteristics, Stability and Short-Wavelength
 Phenomena in Two-Phase Flow Equation Systems"
 ANCR-1272 1976

30. Malecki, I.
 "Physical Foundations of Technical Acoustics"
 Pergamon Press 1969

31. Hueter, T. F. and Bolt, R. H.
 "Sonics"
 John Wiley and Sons, NY 1955

32. Greene, E. F. and Toennies, J. P.
 "Chemical Reactions in Shock Waves"
 Academic Press 1964

33. Zeldovitch, Ya. B. and Raizer, Yu. P.
 "Physics of Shock Waves and High Temperature
 Hydrodynamic Phenomena"
 Academic Press 1966

34. Sears, F. W.
 "Thermodynamics, The Kinetic Theory of Gases,
 and Statistical Mechanics"
 Addison-Wesley 2nd Edition 1959

35. Williams, F. A.
 "Combustion Theory"
 Addison-Wesley 1965

36. Gordon, S. and McBride, B. J.
 "Computer Program for Calculation of Complex Chemical
 Equilibrium Compositions, Rocket Performance, Incident
 and Reflected Shocks, and Chapman-Jouguet Detonations"
 Report No. NASA SP-273 1971

37. Chu, B. T.
 "Wave Propagation in a Reacting Mixture"
 Proc. 1958 Heat Transfer and Fluid Mechanics Institute
 University of California at Berkeley 1958

- 66

- 47 Wallis, G. B.
"One-Dimensional Two-Phase Flow"
McGraw-Hill 1969
- 48 Eddington, R. B.
"Investigation of Supersonic Phenomena in a Two-Phase
(Liquid-Gas) Tunnel"
AIAA J. vol. 8, n. 1, pp. 65-74 January 1970
- 49 Gough, P. S.
"The Flow of a Compressible Gas Through an Aggregate
of Mobile, Reacting Particles"
PhD Thesis, McGill University 1974
- 50 Stuhmiller, J. H. and Ferguson, R. E.
"Calculations of Internal Ballistic Flow with a
Projectile to Wall Gap"
Ballistic Research Laboratory Contract Report
ARBRL-CR-00463 (ADA 104632) August 1981
- 51 Shelton, S., Bergles, A. and Saha, P.
"Study of Heat Transfer and Erosion in Gun Barrels"
AFATL-TR-73-69 March 1973
- 52 Keller, G.
Private Communication
- 53 Westley, F.
"Table of Recommended Rate Constants for Chemical
Reactions Occurring in Combustion"
NSRDS-NBS67 April 1980
- 54 Brupbacher, J. M., Kern, R. D. and O'Grady, B. V.
"Reaction of Hydrogen and Carbon Dioxide Behind
Reflected Shock Waves"
J. Phys. Chem. vol. 80, n. 10, pp. 1031-1035 May 1976
- 55 Keller, G. E. and Schmidt, E. M.
"Gun Muzzle Gas Temperature Measurements Using
Acoustic Thermometry--A Progress Report"
Proceedings of the 17th JANNAF Combustion Meeting 1980
- 56 Gough, P. S.
"The NOVA Code: A User's Manual"
IHCR-80-8 December 1980
- 57 Klingenberg, G. and Mach, H.
"Experimental Study of Non-Steady Phenomena
Associated with the Combustion of Solid Gun Propellants"
16th Symposium on Combustion, MIT August 1976

Nomenclature

a	Speed of sound
b	Covolume
C_i	Molar concentration
C_v	Specific heat at constant volume
C_p	Specific heat at constant pressure
F_p	Drag force exerted on gas by single particle
g_o	Constant to reconcile units of measurement
Im	Imaginary part of complex number
k	Wave number
k_c	Thermal conductivity
n	Number of particles per unit volume
p	Pressure
Re	Real part of complex number
r_p	Radius of a particle
s	Entropy
T	Temperature
t	Time
u	Velocity
x	Position

Greek Symbols

α_i	Volume fraction of phase i
γ	Ratio of specific heats

λ	Second viscosity coefficient
μ	First viscosity coefficient
ν', ν''	Stoichiometric coefficients
ξ	Arbitrary internal variable
ρ	Density
σ	Stress tensor
τ	Relaxation time
Φ	Fourier component
ϕ	Fourier amplitude
ω	Frequency

DISTRIBUTION LIST

<u>No. Of Copies</u>	<u>Organization</u>	<u>No. Of Copies</u>	<u>Organization</u>
12	Administrator Defense Technical Info Center ATTN: DTIC-DDA Cameron Station Alexandria, VA 22314	3	Commander US Army Materiel Development and Readiness Command ATTN: DRCMD-ST DCRSF-E, Safety Office DRCDE-DW 5001 Eisenhower Avenue Alexandria, VA 22333
1	Office of the Under Secretary of Defense Research & Engineering ATTN: R. Thorkildsen Washington, DC 20301	13	Commander US Army Armament R&D Command ATTN: DRDAR-TSS DRDAR-TDC D. Gyorog DRDAR-LCA K. Russell J. Lannon A. Beardell D. Downs S. Einstein L. Schlosberg S. Westley S. Bernstein P. Kemmey G. Heyman Dover, NJ 07801
1	HQDA/SAUS-OR, D. Hardison Washington, DC 20301		
1	HQDA/DAMA-ZA Washington, DC 20310		
2	HODA, DAMA-CSM, A. German E. Lippi Washington, DC 20310		
1	HQDA/SARDA Washington, DC 20310		
1	Commandant US Army War College ATTN: Library-FF229 Carlisle Barracks, PA 17013	9	US Army Armament R&D Command ATTN: DRDAR-SCA, L. Stiefel B. Brodman DRDAR-LCB-I, D. Spring DRDAR-LCE, R. Walker DRDAR-LCU-CT E. Barrieres R. Davitt DRDAR-LCU-CV C. Mandala E. Moore DRDAR-LCM-E S. Kaplowitz Dover, NJ 07801
1	Ballistic Missile Defense Advanced Technology Center P. O. Box 1500 Huntsville, AL 35804		
1	Chairman DOD Explosives Safety Board Room 856-C Hoffman Bldg. 1 2461 Eisenhower Avenue Alexandria, VA 22331		

DISTRIBUTION LIST

<u>No. Of Copies</u>	<u>Organization</u>	<u>No. Of Copies</u>	<u>Organization</u>
5	Commander US Army Armament R&D Command ATTN: DRDAR-QAR, J. Rutkowski Dover, NJ 07801	5	Commander US Army Armament Materiel Readiness Command ATTN: DRSAR-LEP-L, Tech Lib DRSAR-LC, L. Ambrosini DRDAR-IRC, G. Cowan DRSAR-LEM, W. Fortune R. Zastrow Rock Island, IL 61299
5	Project Manager Cannon Artillery Weapons System ATTN: DRCPM-CAWS F. Menke DRCPM-CAWS-WS H. Noble DRCPM-CAWS-SI M. Fisette DRCPM-CAWS-AM R. DeKleine H. Hassmann Dover, NJ 07801	1	Commander US Army Watervliet Arsenal ATTN: SARWV-RD, R. Thierry Watervliet, NY 12189
		1	Director US Army ARRADCOM Benet Weapons Laboratory ATTN: DRDAR-LCB-TL Watervliet, NY 12189
3	Project Manager Munitions Production Base Modernization and Expansion ATTN: DRCPM-PMB, J. Ziegler M. Lohr A. Siklosi Dover, NJ 07801	1	Commander US Army Aviation Research and Development Command ATTN: DRDAV-E 4300 Goodfellow Blvd. St. Louis, MO 63120
3	Project Manager Tank Main Armament System ATTN: DRCPM-TMA, D. Appling DRCPM-TMA-105 DRCPM-TMA-120 Dover, NJ 07801	1	Commander US Army TSARCOM 4300 Goodfellow Blvd. St. Louis MO 63120
		1	Director US Army Air Mobility Research And Development Laboratory Ames Research Center Moffett Field, CA 94035
4	Commander US Army Armament R&D Command ATTN: DRDAR-LCW-A M. Salsbury DRDAR-LCS DRDAR-LCU, A. Moss DRDAR-LC, J. Frasier Dover, NJ 07801		

DISTRIBUTION LIST

<u>No. Of Copies</u>	<u>Organization</u>	<u>No. Of Copies</u>	<u>Organization</u>
1	Commander US Army Communications Research and Development Command ATTN: DRDCO-PPA-SA Fort Monmouth, NJ 07703	1	Project Manager Improved TOW Vehicle ATTN: DRCPM-ITV US Army Tank Automotive Research & Development Command Warren, MI 48090
1	Commander US Army Electronics Research and Development Command Technical Support Activity ATTN: DELSD-L Fort Monmouth, NJ 07703	1	Program Manager M1 Tank System ATTN: DRCPM-GMC-SA, Warren, MI 48090
1	Commander US Army Harry Diamond Lab. ATTN: DELHD-TA-L 2800 Powder Mill Road Adelphi, MD 20783	1	Project Manager Fighting Vehicle Systems ATTN: DRCPM-FVS Warren, MI 48090
2	Commander US Army Missile Command ATTN: DRSMI-R DRSMI-YDL Redstone Arsenal, AL 35898	1	Director US Army TRADOC Systems Analysis Activity ATTN: ATAA-SL, Tech Lib White Sands Missile Range, NM 88002
1	Commander US Army Natick Research and Development Command ATTN: DRDNA-DT, Dr. Sieling Natick, MA 01762	1	Project Manager M-60 Tank Development ATTN: DRCPM-M60TD Warren, MI 48090
1	Commander US Army Tank Automotive Research and Development Command ATTN: DRDTA-UL Warren, MI 48090	1	Commander US Army Training & Doctrine Command ATTN: ATCD-MA/ MAJ Williams Fort Monroe, VA 23651
1	US Army Tank Automotive Materiel Readiness Command ATTN: DRSTA-CG Warren, MI 48090	2	Commander US Army Materials and Mechanics Research Center ATTN: DRXMR-ATL Tech Library Watertown, MA 02172

DISTRIBUTION LIST

<u>No. Of Copies</u>	<u>Organization</u>	<u>No. Of Copies</u>	<u>Organization</u>
1	Commander US Army Research Office ATTN: Tech Library P. O. Box 12211 Research Triangle Park, NC 27709	1	Commander US Army Foreign Science & Technology Center ATTN: DRXST-MC-3 220 Seventh Street, NE Charlottesville, VA 22901
1	Commander US Army Mobility Equipment Research and Development Command ATTN: DRDME-WC Fort Belvoir, VA 22060	1	President US Army Artillery Board Ft. Sill, OK 73504
1	Commander US Army Logistics Mgmt Ctr Defense Logistics Studies Fort Lee, VA 23801	2	Commandant US Army Field Artillery School ATTN: ATSF-CO-MW, B. Willis Ft. Sill, OK 73503
1	Commandant US Army Infantry School ATTN: Infantry Agency Fort Benning, GA 31905	3	Commandant US Army Armor School ATTN: ATZK-CD-MS M. Falkovitch Armor Agency Fort Knox, KY 40121
1	US Army Armor & Engineer Board ATTN: STEBB-AD-S Fort Knox, KY 40121	1	Chief of Naval Materiel Department of the Navy ATTN: J. Amlie Washington, DC 20360
1	Commandant US Army Aviation School ATTN: Aviation Agency Fort Rucker, AL 36360	1	Office of Naval Research ATTN: Code 473, R. S. Miller 800 N. Quincy Street Arlington, VA 22217
1	Commandant Command and General Staff College Fort Leavenworth, KS 66027	2	Commander Naval Sea Systems Command ATTN: SEA-62R, J. W. Murrin R. Beauregard National Center, Bldg. 2 Room 6E08 Washington, DC 20362
1	Commandant US Army Special Warfare School ATTN: Rev & Tng Lit Div Fort Bragg, NC 28307	1	Commander Naval Air Systems Command ATTN: NAIR-954-Tech Lib Washington, DC 20360
1	Commandant US Army Engineer School ATTN: ATSE-CD Ft. Belvoir, VA 22060		

DISTRIBUTION LIST

<u>No. Of Copies</u>	<u>Organization</u>	<u>No. Of Copies</u>	<u>Organization</u>
1	Strategic Systems Project Office Dept. of the Navy Room 901 ATTN: J. F. Kincaid Washington, DC 20360	4	Commander Naval Weapons Center ATTN: Code 388, R. L. Derr C. F. Price T. Boggs Info. Sci. Div. China Lake, CA 93555
1	Assistant Secretary of the Navy (R, E, and S) ATTN: R. Reichenbach Room 5E787 Pentagon Bldg. Washington, DC 20350	2	Superintendent Naval Postgraduate School Dept. of Mechanical Engineering ATTN: A. E. Fuhs Code 1424 Library Monterey, CA 93940
1	Naval Research Lab Tech Library Washington, DC 20375	6	Commander Naval Ordnance Station ATTN: P. L. Stang J. Birkett S. Mitchell C. Christensen D. Brooks Tech Library Indian Head, MD 20640
5	Commander Naval Surface Weapons Center ATTN: Code G33, J. L. East D. McClure W. Burrell J. Johndrow Code DX-21 Tech Lib Dahlgren, VA 22448	1	AFSC/SDOA Andrews AFB Washington, DC 20331
2	Commander US Naval Surface Weapons Center ATTN: J. P. Consaga C. Gotzmer Indian Head, MD 20640	1	Program Manager AFOSR Directorate of Aerospace Sciences ATTN: L. H. Caveny Bolling AFB, DC 20332
4	Commander Naval Surface Weapons Center ATTN: S. Jacobs/Code 240 Code 730 K. Kim/Code R-13 R. Bernecker Silver Spring, MD 20910	6	AFRPL (DYSC) ATTN: D. George J. N. Levine B. Goshgarian D. Thrasher N. Vander Hyde Tech Library Edwards AFB, CA 93523
2	Commanding Officer Naval Underwater Systems Center Energy Conversion Dept. ATTN: CODE 5B331, R. S. Lazar Tech Lib Newport, RI 02840		

DISTRIBUTION LIST

<u>No. Of Copies</u>	<u>Organization</u>	<u>No. Of Copies</u>	<u>Organization</u>
1	AFFTC ATTN: SSD-Tech Lib Edwards AFB, CA 93523	1	AVCO Everett Rsch Lab ATTN: D. Stickler 2385 Revere Beach Parkway Everett, MA 02149
1	AFATL ATTN: DLYV Eglin AFB, FL 32542	2	Calspan Corporation ATTN: E. B. Fisher Tech Library P. O. Box 400 Buffalo, NY 14225
1	AFATL/DL DL ATTN: O. K. Heiney Eglin AFB, FL 32542		
1	ADTC ATTN: DLODL Tech Lib Eglin AFB, FL 32542	1	Foster Miller Associates ATTN: A. Erickson 135 Second Avenue Waltham, MA 02154
1	AFFDL ATTN: TST-Lib Wright-Patterson AFB, OH 45433	1	Atlantic Research Corp. ATTN: M. K. King 5390 Cherokee Ave. Alexandria, VA 22314
1	NASA HQ 600 Independence Avenue, SW ATTN: Code JM6, Tech Lib. Washington, DC 20546	1	General Applied Sciences Lab ATTN: J. Erdos Merrick & Stewart Avenues Westbury Long Island, NY 11590
1	NASA/Lyndon B. Johnson Space Center ATTN: NHS-22, Library Section Houston, TX 77058	1	General Electric Company Armament Systems Dept. ATTN: M. J. Bulman, Room 1311 Lakeside Avenue Burlington, VT 05412
1	Aerodyne Research, Inc. Bedford Research Park ATTN: V. Yousefian Bedford, MA 01730	1	Hercules, Inc. Allegheny Ballistics Laboratory ATTN: R. B. Miller P. O. Box 210 Cumberland, MD 21501
1	Aerojet Solid Propulsion Co. ATTN: P. Micheli Sacramento, CA 95813	1	Hercules, Inc Bacchus Works ATTN: K. P. McCarty P. O. Box 98 Magna, UT 84044

DISTRIBUTION LIST

<u>No. Of Copies</u>	<u>Organization</u>	<u>No. Of Copies</u>	<u>Organization</u>
1	Hercules, Inc. Eglin Operations AFATL DLDL ATTN: R. L. Simmons Eglin AFB, FL 32542	2	Rockwell International Rocketdyne Division ATTN: BA08 J. E. Flanagan J. Grey 6633 Canoga Avenue Canoga Park, CA 91304
1	IITRI ATTN: M. J. Klein 10 W. 35th Street Chicago, IL 60616	1	Science Applications, Inc. ATTN: R. B. Edelman 23146 Cumorah Crest Woodland Hills, CA 91364
2	Lawrence Livermore Laboratory ATTN: M. S. L-355, A. Buckingham M. Finger P. O. Box 808 Livermore, CA 94550	1	Scientific Research Assoc., Inc. ATTN: H. McDonald P. O. Box 498 Glastonbury, CT 06033
1	Olin Corporation Badger Army Ammunition Plant ATTN: R. J. Thiede Baraboo, WI 53913	1	Shock Hydrodynamics, Inc. ATTN: W. H. Andersen 4710-16 Vineland Avenue North Hollywood, CA 91602
1	Olin Corporation Smokeless Powder Operations ATTN: R. L. Cook P. O. Box 222 ST. Marks, FL 32355	3	Thiokol Corporation Huntsville Division ATTN: D. Flanigan R. Glick Tech Library Huntsville, AL 35807
1	Paul Gough Associates, Inc. ATTN: P. S. Gough P. O. Box 1614 Portsmouth, NH 03801	2	Thiokol Corporation Wasatch Division ATTN: J. Peterson Tech Library P. O. Box 524 Brigham City, UT 84302
1	Physics International Company 2700 Merced Street Leandro, CA 94577	2	Thiokol Corporation Elkton Division ATTN: R. Biddle Tech Lib. P. O. Box 241 Elkton, MD 21921
1	Princeton Combustion Research Lab., Inc. ATTN: M. Summerfield 1041 US Highway One North Princeton, NJ 08540		
1	Pulsepower Systems, Inc. ATTN: L. C. Elmore 815 American Street San Carlos, CA 94070		

DISTRIBUTION LIST

<u>No. Of Copies</u>	<u>Organization</u>	<u>No. Of Copies</u>	<u>Organization</u>
2	United Technologies Chemical Systems Division ATTN: R. Brown Tech Library P. O. Box 358 Sunnyvale, CA 94086	1	University of Massachusetts Dept. of Mechanical Engineering ATTN: K. Jakus Amherst, MA 01002
1	Universal Propulsion Company ATTN: H. J. McSpadden Black Canyon Stage 1 Box 1140 Phoenix, AZ 85029	1	University of Minnesota Dept. of Mechanical Engineering ATTN: E. Fletcher Minneapolis, MN 55455
1	Southwest Research Institute Institute Scientists ATTN: Robert E. White 8500 Culebra Road San Antonio, TX 78228	1	Case Western Reserve University Division of Aerospace Sciences ATTN: J. Tien Cleveland, OH 44135
1	Battelle Memorial Institute ATTN: Tech Library 505 King avenue Columbus, OH 43201	3	Georgia Institute of Tech School of Aerospace Eng. ATTN: B. T. Zinn E. Price W. C. Strahle Atlanta, GA 30332
1	Brigham Young University Dept. of Chemical Engineering ATTN: M. Beckstead Provo, UT 84601	1	Institute of Gas Technology ATTN: D. Gidaspow 3424 S. State Street Chicago, IL 60616
1	California Institute of Tech 204 Karman Lab Main Stop 301-46 ATTN: F. E. C. Culick 1201 E. California Street Pasadena, CA 91125	1	Johns Hopkins University Applied Physics Laboratory Chemical Propulsion Information Agency ATTN: T. Christian Johns Hopkins Road Laurel, MD 20707
1	California Institute of Tech Jet Propulsion Laboratory 4300 Oak Grove Drive Pasadena, CA 91103	1	Massachusetts Institute of Tech Dept of Mechanical Engineering ATTN: T. Toong Cambridge, MA 02139
1	University of Illinois Dept of Mech Eng ATTN: H. Krier 144 MEB, 1206 W. Green Street Urbana, IL 61801		

DISTRIBUTION LIST

<u>No. Of Copies</u>	<u>Organization</u>	<u>No. Of Copies</u>	<u>Organization</u>
1	Pennsylvania State University Applied Research Lab ATTN: G. M. Faeth P. O. Box 30 State College, PA 16801	1	University of Southern California Mechanical Engineering Dept. ATTN: OHE200, M. Gerstein Los Angeles, CA 90007
1	Pennsylvania State University Dept. Of Mechanical Engineering ATTN: K. Kuo University Park, PA 16802	2	University of Utah Dept. of Chemical Engineering ATTN: A. Baer G. Flandro Salt Lake City, UT 84112
1	Purdue University School of Mechanical Engineering ATTN: J. R. Osborn TSPC Chaffee Hall West Lafayette, IN 47906	1	Washington State University Dept. of Mechanical Engineering ATTN: C. T. Crowe Pullman, WA 99163
1	Rensselaer Polytechnic Inst. Department of Mathematics Troy, NY 12181		<u>Aberdeen Proving Ground</u> Dir, USAMSAA ATTN: DRXSY-D DRXSY-MP, H. Cohen Cdr, USATECOM ATTN: DRSTE-TO-F STEAP-MT, S. Walton G. Rice D. Lacey C. Herud
1	Rutgers University Dept. of Mechanical and Aerospace Engineering ATTN: S. Temkin University Heights Campus New Brunswick, NJ 08903		Dir, HEL ATTN: J. Weisz Dir, USACSL, Bldg. E3515, EA ATTN: DRDAR-CLB-PA
1	SRI International Propulsion Sciences Division ATTN: Tech Library 333 Ravenswood Avenue Menlo Park, CA 94025		
1	Stevens Institute of Technology Davidson Laboratory ATTN: R. McAlevy, III Hoboken, NJ 07030		
2	Los Alamos Scientific Lab ATTN: Thomas D. Butler MS B126 M. Division, B. Craig P. O. Box 1663 Los Alamos, NM 87545		

USER EVALUATION OF REPORT

Please take a few minutes to answer the questions below; tear out this sheet, fold as indicated, staple or tape closed, and place in the mail. Your comments will provide us with information for improving future reports.

1. BRL Report Number _____
2. Does this report satisfy a need? (Comment on purpose, related project, or other area of interest for which report will be used.)

3. How, specifically, is the report being used? (Information source, design data or procedure, management procedure, source of ideas, etc.) _____

4. Has the information in this report led to any quantitative savings as far as man-hours/contract dollars saved, operating costs avoided, efficiencies achieved, etc.? If so, please elaborate.

5. General Comments (Indicate what you think should be changed to make this report and future reports of this type more responsive to your needs, more usable, improve readability, etc.) _____

6. If you would like to be contacted by the personnel who prepared this report to raise specific questions or discuss the topic, please fill in the following information.

Name: _____

Telephone Number: _____

Organization Address: _____

